Palaeobiodiversity and Palaeoenvironments (2025) 105:343–375
https://doi.org/10.1007/s12549-025-00664-3

SENCKENBERG

ORIGINAL PAPER

Palaeocene herpetofauna of Walbeck (Sachsen-Anhalt, Germany) with a focus on lissamphibians

Davit Vasilyan[1,2] · **Loredana Macaluso**[3,4]

Received: 26 August 2024 / Revised: 12 May 2025 / Accepted: 15 May 2025 / Published online: 10 July 2025

Abstract

The Palaeocene Epoch is one of the most enigmatic intervals in Earth history, due to its limited fossil record. Lasting only 10 Ma, the Palaeocene is a transitional interval between the Mesozoic and Cenozoic eras when most extant vertebrate clades either appeared or, if they originated earlier, continued diversifying. Whereas the mammalian fauna from the Palaeocene of Europe is relatively well understood, other continental vertebrate groups such as amphibians and reptiles are not. In the present paper, we describe the non-squamate portion of the herpetofauna from the Walbeck site (early–middle Palaeocene or MP 1–5, Germany) with a special focus on the lissamphibians. The Walbeck fossil amphibian and reptile collection was considered lost for many decades. The recent rediscovery of this historically significant collection means its temporally important herpetofauna can be reevaluated. We redescribe and provide emended diagnoses for the three previously named salamander species: *Wolterstorffiella wiggeri, Geyeriella mertensi* and *Koalliella genzeli.* Phylogenetic analysis of the three salamander species suggests an unclear salamandroid affiliation for the large-sized *Wolterstorffiella*, whereas the small-sized *Geyeriella* and *Koalliella* are assigned to the families Proteidae and Salamandridae, respectively. For the first time, we describe the Walbeck frog fauna, which includes Palaeobatrachidae indet., a new alytid genus and species and a pelobatid (?*Eopelobates*). The pelobatid is the oldest record for the family in Europe. We also report on some non-diagnostic bones of a crocodile and a turtle, which, along with recently reported lizard fossils, lead to a fuller understanding of the Walbeck reptilian fauna. Thanks to its early–middle Palaeocene age and diversity of taxa, the Walbeck site provides insights into the earliest Cenozoic history of amphibians and reptiles in Europe. The Walbeck herpetofauna includes: 1) taxa known exclusively from the Palaeocene of Europe (salamandroid *Wolterstorffiella*, new alytid and lacertoid *Camptognathosaurus*), 2) the first European appearances of the extant families Proteidae (*Geyeriella*), Salamandridae (*Koalliella*), Pelobatidae and Lacertidae, and 3) continuing records for two families (Palaeobatrachidae and Alytidae) that have their roots in the European Mesozoic.

Keywords Frogs · Germany · Lissamphibian · Salamanders · Palaeocene · Walbeck

This article is a contribution to the special issue "Festschrift for Márton Venczel"

This article is registered in Zoobank under https://zoobank.org/References/6235C31D-CEDB-4FEE-869D-F1AA8BAC7EB5

✉ Davit Vasilyan
davit.vasilyan@jurassica.ch

[1] JURASSICA Museum, Route de Fontenais 21, 2900 Porrentruy, Switzerland

[2] Department of Geosciences, University of Fribourg, Chemin du musée 6, 1700 Fribourg, Switzerland

[3] Regional Museum of Natural Sciences, Via Giolitti 36, 10123 Turin, Italy

[4] Natural Sciences Collections, Martin Luther University Halle-Wittenberg, Domplatz 4, 06108 Halle (Saale), Germany

Introduction

The Palaeocene Epoch is one of the most obscure intervals in the history of vertebrates. Following the K-Pg extinction event and lasting only 10 Ma (Gradstein and Ogg 2020), it marks the beginning of the age of mammals and is characterised by the coexistence of both archaic (Mesozoic survivors) and new clades replacing Mesozoic taxa (e.g. Roček 2013). The Palaeocene continental vertebrate record is limited, and not many fossil sites are known. Whereas Palaeocene mammals are the most frequently found and studied group, amphibians and reptiles are less studied groups. For the few known European Palaeocene vertebrate sites, amphibians and reptiles have been reported or described in only half of them (Fig. 1). This fact makes any sites with amphibian

Fig. 1 Palaeogeographic map of Europe during the Palaeocene Epoch with an outline of the present-day European continent, redrawn from De Bast and Smith (2016), and indicating Palaeocene vertebrate sites

and reptile fossils exceptionally valuable for documenting and interpreting Palaeocene herpetofaunas of Europe. Although most of those sites have been known for decades, their amphibians and reptiles received less attention, either because of the fragmentary nature of the material (e.g. Cernay: Estes et al. 1967; Hainin: e.g. Groessens-Van Dyck 1981a, b) or after their first description(s), the material was reportedly lost (Walbeck: Estes 1981).

The present work is dedicated to the study of the herpetofauna of the Walbeck site, with a special focus on the salamander and frog record. Lissamphibian material was previously considered to be lost (Estes 1981). However, the Walbeck collection recently was rediscovered in the palaeontological collection at the University of Halle. The Walbeck site represents a karstic pocket in Triassic (Muschelkalk) limestone, which had been fully excavated in the beginning of the 20th century (e.g. Weigelt 1939). Based on its mammalian fauna, the assemblage has been correlated to the European Palaeogene mammalian reference interval MP 1–5 (De Bast et al. 2013; De Bast and Smith 2016), or early–middle Palaeocene. The material is entirely composed of disarticulated, isolated bones. Along with mammals, the Walbeck vertebrate fauna includes amphibians, reptilians, and avians. Some of those groups have been previously studied (e.g. Herre 1939; Kuhn 1940; Weigelt 1942) and recently revised (Mayr 2002, 2007; Storch 2008; Čerňanský and Vasilyan 2024).

Among the Walbeck amphibians, only the salamanders have been studied and published (Herre 1939, 1950). In the first report on salamanders from Walbeck, Herre (1939) erected the new genus *Wolterstorffiella*, without providing a species name. He also figured and discussed (Herre 1939: fig. 2) another two small-sized isolated vertebrae without naming them. Later, these two vertebrae, together with further material, were described as the new genus and species *Geyeriella mertensi* (Herre 1950). In the same work, Herre (1950) also described two additional new genera and species, *Wolterstorffiella wiggeri* and *Koalliella genzeli*, both based on isolated vertebrae. After these studies, the salamander remains were considered lost (e.g. Estes 1981), making it difficult to revise and compare those taxa and fossils with other salamanders, because the original publications provided only incomplete descriptions and the material was not adequately figured. The recent rediscovery of most of the specimens described by Herre (1950) allows a redescription of this material and the inclusion of these taxa in a phylogenetic framework. Along with salamanders, we also discovered previously unreported bones of frogs, which we describe herein for the first time.

Material and methods

The studied specimens from Walbeck are all housed at the Institut für Geologische Wissenschaften und Geiseltalmuseum, Martin-Luther-Universität Halle-Wittenberg, Halle, Germany. The fossils were photographed using a Keyence VHX970 digital light microscope at the JURASSICA Museum, Porrentruy, Switzerland.

The bone nomenclature of salamanders follows Venczel and Codrea (2018) and Macaluso et al. (2023). Two new anatomical terms for the description of the salamander atlas are introduced in the present work: dorsal and ventral alar processes. The latter corresponds to the alar-like process sensu Venczel and Codrea (2018). Nomenclature for frog bones is as follows: frontoparietal – Roček (1981); ilia – Gómez and Turazzini (2015); maxilla – Villa et al. (2016); radioulna – Keeffe and Blackburn (2022); sphenethmoid – Vasilyan et al. (2017); vertebrae – Sanchiz (1998a). Given the complex taxonomic history of the material and the fact that we provide a systemic revision of the materials described by Herre (1950), specimens in our paper are figured based on taxonomic criteria (lectotype or neotype figured first, followed by paralectotypes, and finally by referred material), rather than in the conventional anatomical order.

Apart from literature sources, the following extant specimens were also used for comparisons: *Ambystoma tigrinum* (MDHC 88, MDHC 209), *Cynops orientalis* (MDHC 397), *Tylototriton verrucosus* (MDHC 251), *Rhyacotriton variegatus* (MVZ 98409; AmphibiaTree 2007), *Dicamptodon ensatus* (MVZ 69449; Wake 2001).

Selected elements were studied using computed tomography. µCT data were obtained using the Bruker Skyscanner 2211 at the Univertsité de Fribourg, Switzerland, with the following settings: 18 µm resolution, 664 mA, 65 kV, without filter. The tomographic reconstruction was performed using Nricon Software, Univerisité de Fribourg, Switzerland. The visualization and segmentation were performed using Amira 9.0 software in Porrentruy, Switzerland.

Phylogenetic analysis

To evaluate the phylogenetic position of the salamander taxa, we conducted an analysis based on the vertebrae-based character matrix published by Skutschas et al. (2024), which is an update of the matrix originally created by DeMar (2013). Our character list follows Macaluso et al. (2022a). We added five extant species (*Ambystoma tigrinum*, *Dicamptodon enstatus*, *Lissotriton helveticus*, *Rhyacotriton variegatus, Salamandrella keyserlingii*), and some scorings were modified and improved (see Appendix S1). Phylogenetic scorings for *Li. helveticus* and *S. keyserlingii* are based on Macaluso et al. (2023). Our matrix includes 24 taxa and 27 characters.

To clarify the phylogenetic affinities of *Koalliella* among Salamandridae, we analyzed this taxon using a second character matrix focusing on the family Salamandridae of Macaluso et al. (2023). Our character list follows Macaluso et al. (2023) and our character-taxon matrix is presented in Appendix S2. This second dataset includes 14 genus-level operational taxonomic units and 83 osteological characters related to the occipito-otic (sensu Rose 2003) and the vertebrae. Both character-taxon matrices were manipulated using Mesquite v.3.61 (Maddison and Maddison 2023). The phylogenetic analyses were run using TNT v1.6 (Goloboff et al. 2008) using the Traditional Search with 1000 repetitions set.

Institutional abbreviations

DE, Department of Ecology, Comenius University in Bratislava, Slovakia;
ISEZ FR/WI, Institute of Systematics and Evolution of Animals, Polish Academy of Sciences Kraków, Poland, Węże I collection;
MDHC, Massimo Delfino's Herpetological Collection, housed in the Department of Earth Science of Turin, Italy;
MLU, Martin-Luther-Universität Halle-Wittenberg, Halle, Germany;
MVZ, University of California Museum of Vertebrate Zoology, Berkeley, U.S.A.;
NHMW, Museum of Natural History, Vienna, Austria;
ZSM, The Bavarian State Collection of Zoology, Munich, Germany.

Systematic palaeontology

Amphibia Linnaeus, 1758
Lissamphibia Haeckel, 1866
Caudata Scopoli, 1777
Salamandroidea Noble, 1931
Wolterstorffiella Herre, 1950

Wolterstorffiella wiggeri Herre, 1950
(Fig. 2)

Taxonomic note: The genus name *Wolterstorffiella* was first mentioned by Herre (1939) in reference to at least four vertebrae. However, in that work, neither a type species nor a holotype was designated, and no description was provided. Among them, only one vertebra, MLU.GeoS.4081, could be identified by us in Herre's (1939: fig. 1) account. The species *W. wiggeri* was named and described later by Herre (1950), where appropriate designations of the type material and type species were provided; thus Herre (1950) should be considered as the taxonomic authority for both the genus and species names.

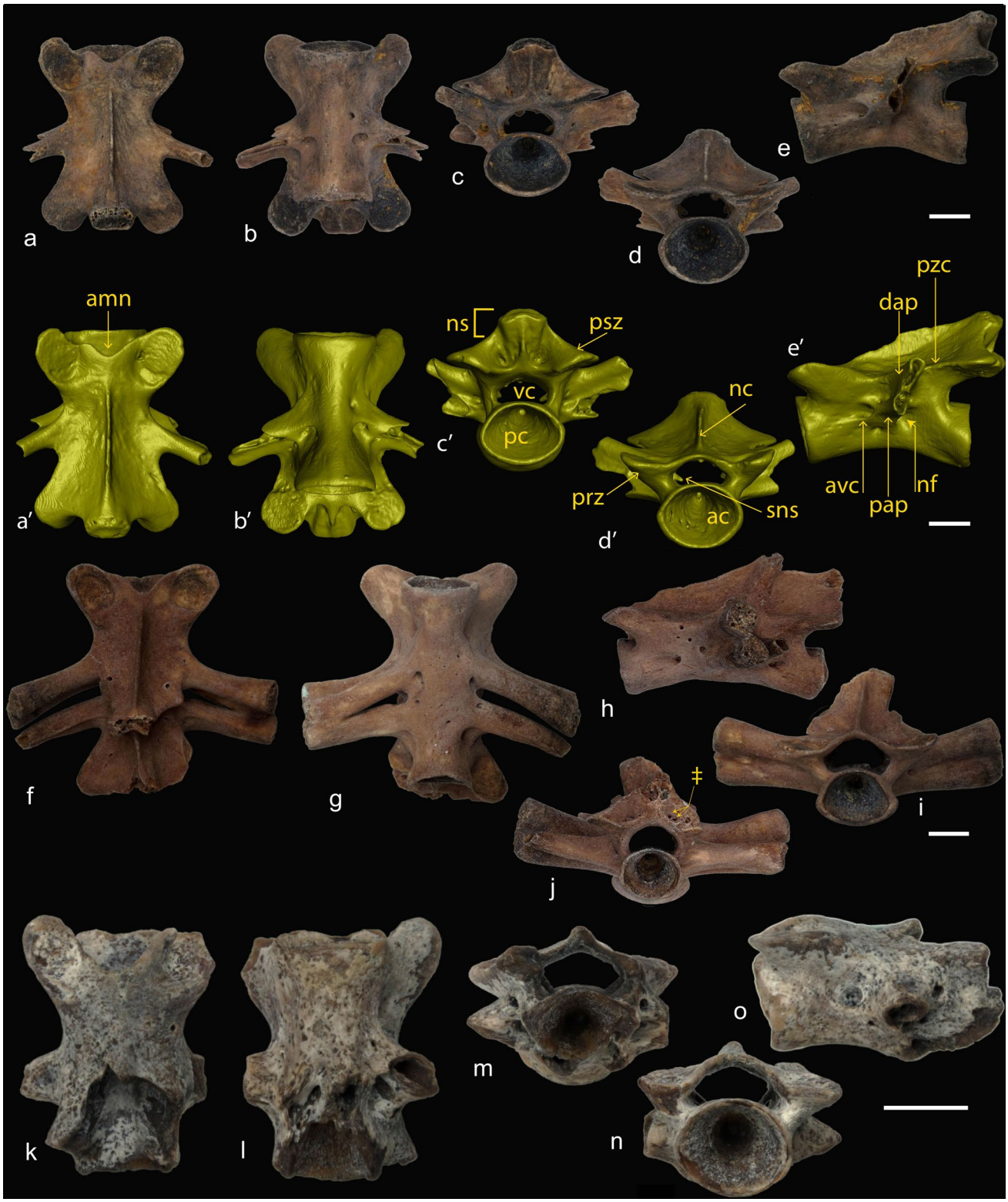
a
b
c
d
e
amn
a′
b′
ns
psz
vc
pc
c′
nc
prz
ac
sns
d′
pzc
dap
e′
avc
pap
nf
f
g
h
‡
i
j
k
l
m
n
o

◂ **Fig. 2** Photographs (**a**–**e**, **f**–**s**, **v**–**z**) and 3D-models (**a'**–**e'**, **t'**–**u'**, **v'**–**z'**) of the lectotype and selected paralectotype and referred vertebrae of *Wolterstoffiella wiggeri* Herre, 1950 from Walbeck. **a**–**e'** MLU.GeoS.4071 (lectotype), trunk vertebra, entire specimen in dorsal (**a**, **a'**), ventral (**b**, **b'**), posterior (**c**, **c'**), anterior (**d**, **d'**) and left lateral (**e**, **e'**) views. **f**–**j** MLU.GeoS.4070 (paralectotype) fused sacral+postsacral vertebrae, entire specimen in dorsal (**f**), ventral (**g**), left lateral (**h**), anterior (**i**) and posterior (**j**) views; ‡ (**j**) indicates foramina to either side of midline in posteroventral surface of neural spine. **k**–**o** MLU.GeoS.4081 (referred), postsacral (caudosacral or caudal) vertebra, entire specimen in dorsal (**k**), ventral (**l**), posterior (**m**), anterior (**n**), and left lateral (**o**) views. **p**–**s** close–ups of postatlantal vertebrae showing variable condition of spinal nerve foramina: **p** MLU.GeoS.4070 (paralectotype), fused sacral+first caudosacral vertebrae, in right lateral and slightly posteroventral view, showing large spinal foramen in postsacral; **q** MLU.GeoS.4071 (lectotype), trunk vertebra, in left lateral and slightly posterior view, showing small spinal foramen; **r** MLU.GeoS.4077 (paralectotype), postsacral (caudosacral or caudal) vertebra, in right lateral and slightly posterodorsal view, showing large spinal foramen; and **s**, MLU.GeoS.4073 (paralectotype), trunk vertebra, in right lateral and posterior view, lacking spinal nerve foramen. **t**, **u** MLU.GeoS.4071 (lectotype), trunk vertebra, digitally sectioned sagittally (**t**) to show spinal foramen and spinal nerve support in medial surface of left side and entire specimen (**u**) in right lateral, posterior and slightly ventral view to show external exit for spinal foramen. **v**–**z'** MLU.GeoS.4069 (referred), atlas, entire specimen in dorsal (**v**, **v'**), ventral (**w**, **w'**), posterior (**x**, **x'**), anterior (**y**, **y'**) and right lateral and anteroventral (**y''**) views, digitally sectioned sagittally (**y***) to show spinal foramen and spinal nerve support in medial surface of right side and entire specimen (**z**, **z'**) in left lateral view; black dashed line (**y''**) indicates margins of the anterior articular surface on the left anterior cotyle and onto adjacent portion of the odontoid process. Abbreviations: *aas* anterior articular surface; *ac* anterior cotyle; *amn* anteromedial notch; *avc* anterior ventral crest; *dap* diapophysis; *fsn* foramen for spinal nerve; *nc* neural crest; *nf* nutritive foramen; *ns* neural spine; *op* odontoid process; *pap* parapophysis; *pc* posterior cotyle; *prz* prezygapophysis; *psz* postzygapophysis; *pzc* posterior zyg-apophyseal crest; *sns* spinal nerve support; *vc* vertebral canal. Specimens at different magnifications; see corresponding 2 mm scale bars

Emended diagnosis: Robust atlas with the combination of: long centrum bearing short odontoid process; neural crest high and heavily sculptured with pits; single and continuous anterior articulation surface, going from one cotyle wrapping around the ventral surface of the odontoid process and continuing onto other cotyle without interruption. Amphicoelous trunk vertebrae with the combination of: dorsoventrally compressed vertebral canal (narrower and lower than the cotyles); large foramen for blood vessels at the base of parapophyses; bicipital transverse processes consisting of hollow diapophyses and parapophyses; neural spine terminating with porous bone (which indicates it ended in cartilage); the base of transverse processes, between parapophysis and diapophysis, pierced by one to five foramina (never smooth). One to five foramina are always present to either side of the midline on the posteroventral surface of the neural spine, but this character might have a certain degree of variability.

Apomorphies: Two characters based on the matrix of Skutschas et al. (2024): anterior end of neural crest of the atlas in dorsal view is laterally emarginate (ch. 7) and articular surface of odontoid process and anterior cotyles are confluent (ch. 12).

Lectotype: One trunk vertebra, MLU.GeoS.4071 (Fig. 2a–e', q, t, u). Previously designated as lectotype by Estes (1981: p. 49) and depicted by Herre (1950: fig. 1), both without providing an institutional specimen number.

Paralectotypes: Ten trunk vertebrae: MLU.GeoS.4032, MLU.GeoS.4072, MLU.GeoS.4073 (Fig. 2s), MLU.GeoS.4074 (Herre 1950: fig. 3), MLU.GeoS.4075, MLU.GeoS.4076, MLU.GeoS.4078, MLU.GeoS.4079 (Herre 1950: fig. 4), MLU.GeoS.4080 and MLU.GeoS.4082. One fused sacral+first caudosacral vertebrae, MLU.GeoS.4070 (Herre 1950: fig. 2; Fig. 2f–j, p). One postsacral (caudosacral or caudal) vertebra, MLU.GeoS.4077 (Herre 1950: fig. 5; Fig. 2r).

Referred material: Material not mentioned by Herre (1950): one atlas, MLU.GeoS.4069 (Fig. 2v–z') and one postsacral (either caudosacral or caudal) vertebra, MLU.GeoS.4081 (Fig. 2k–o).

Description and remarks

Trunk vertebrae: The centrum of the trunk vertebrae (Fig. 2a–e', t, u) is amphicoelous and in lateral view is ventrally concave. The vertebrae are moderately large, with a centrum length of 6–12 mm. In dorsal view, the vertebra is slightly hourglass-shaped, only slightly narrowing anterior to the diapophyses (Fig. 2a, a'). The centrum is slightly dorsoventrally compressed. The notochordal foramen is clearly visible at or slightly above the centre of the cotyles. The vertebral canal is narrower and lower than the cotyles and strongly dorsoventrally compressed (Fig. 2c, d, c', d'). The anterior ventral crests are short, whereas the posterior ventral crests are absent. Because the posterior ventral crests are absent, the nutritive foramina for the blood vessels that perforate the base of the parapophyses are visible in ventral view, posterior to the transverse processes (Fig. 2e', u). The nutritive foramina are wider in posterior view and narrower in anterior view. The transverse processes are often broken because they are mostly thin-walled and fragile, consisting of hollow diapophyses and parapophyses either united by a lamina or contacting each other. The parapophyses contact only partially the centrum in their dorsal part. The diapophysis seems slightly smaller than the parapophysis (Fig. 2e, e'). One to three foramina perforate the neural arch anterior to the transverse processes, at mid-height between the diapophyses and parapophyses (Fig. 2e'). The centrum and lateral walls of the neural arch have smooth surfaces. The anterior zygapophyseal crests are absent, whereas the posterior zygapophyseal crests sometimes connect the postzygapophyses with the diapophyses (Fig. 2e'). Where present, foramina for the spinal nerve are visible in the inner surface of the vertebral canal and seem to exit posterior to the diapophyses in most of the vertebrae (Fig. 2u). The spinal foramen exits on the lateral

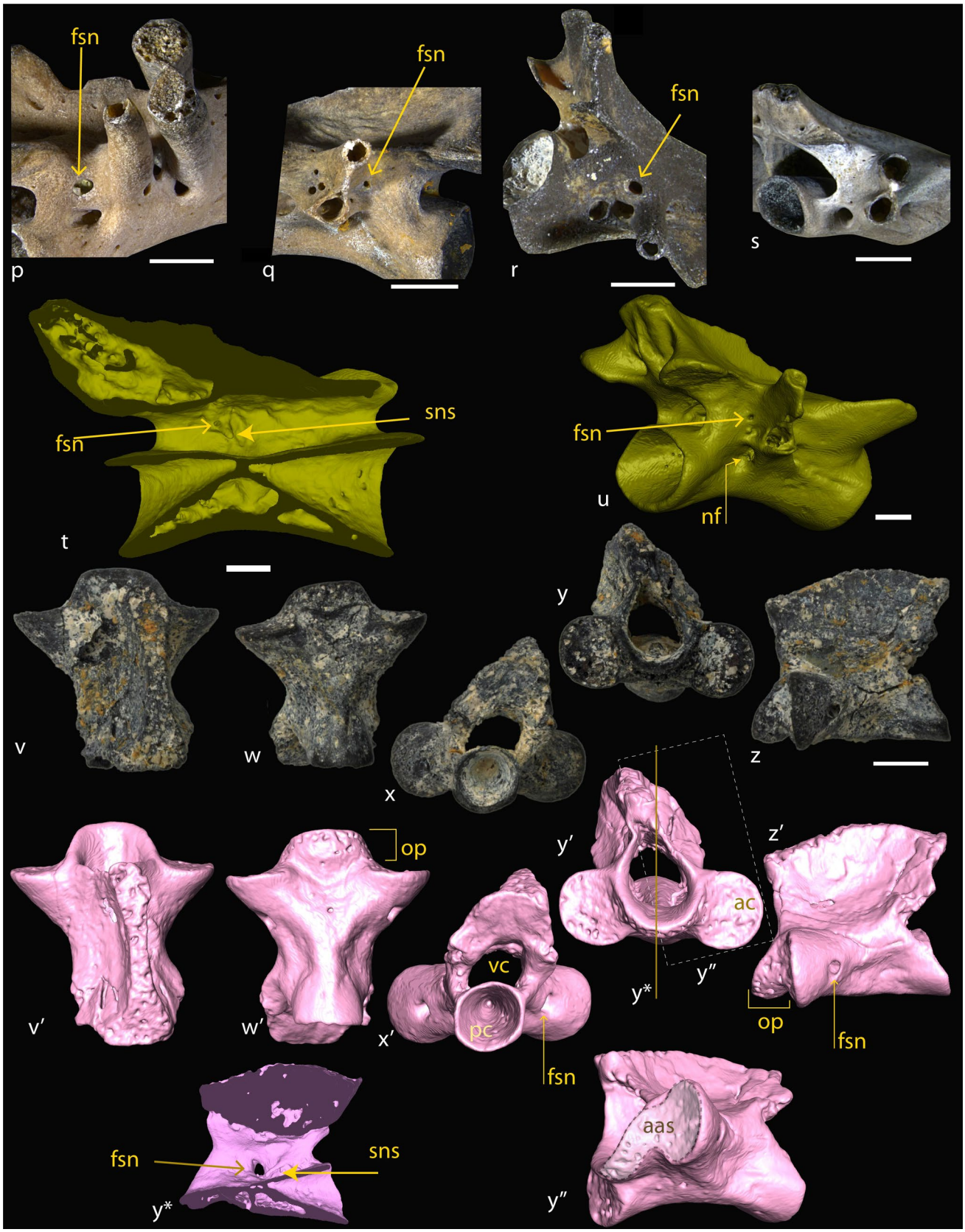

Fig. 2 (continued)

wall of the vertebral canal, posterodorsal to the spinal nerve support (Fig. 2t). In some vertebrae, however, the perforation is not complete, and the foramina are present either only in the inner surface of the neural arch (i.e. MLU.GeoS.4073 (Fig. 2s) and in the right wall of MLU.GeoS.4074) or only in the external surface (i.e. MLU.GeoS.4071 (Fig. 2q) and in the right wall of MLU.GeoS.4079). In two specimens, MLU.GeoS.4072 and MLU.GeoS.4082, spinal foramina seem to be absent both in the inner and outer surfaces of the vertebral canal. These foramina are small and perforate the vertebral canal slightly posterior to the transverse processes. The prezygapophyses are subhorizontal, slightly dorsally concave, and in dorsal view project slightly laterally. In dorsal view, the anterior margin of the neural arch is concave (Fig. 2a'). The anterior end of the neural crest arises at different positions, but is always somewhere between slightly behind the anterior margin of the neural arch and usually not posterior to the mid-length of the vertebra (Fig. 2a, a', f). The neural crest is low to moderately high, and if high, rises gradually posteriorly. It is sharp and slightly broadens posteriorly in proximity to the neural spine. The neural spine is a moderately high, posterodorsal bulge (or posteromedial notch sensu Blain et al. 2011) that terminates in porous bone for the attachment of cartilage (Fig. 2a, a'). In posterior view (e.g. MLU.GeoS.4071; Fig. 2c), the posterior surface of the neural spine bears a sharp crest along its midline. Laterally the crest is surrounded by two concavities that house one to five foramina (Fig. 2j). In other specimens, the crest, concavities, and foramina have different degrees of development. The ventral surface of the centrum is generally smooth, and consistently lacks a subcentral keel or basapophyses.

Fused sacral and first caudosacral vertebrae: A special case is represented by MLU.GeoS.4070 (Herre 1950: fig. 2; Fig. 2f–i), which is composed of two fused vertebrae. In this specimen, the anterior vertebra has complete transverse processes, with dia- and parapophyses contacting each other. The posterior vertebra has unicipital transverse processes. On the right side, the parapophyses of the anterior vertebra and transverse process of the posterior vertebra are fused. Based on the thick (and not hollow) transverse processes of the anterior vertebra and on the unicipital transverse processes of the posterior one (see below), we interpret this specimen as the sacral and first caudosacral vertebrae, which fused most likely as a result of an aberrant development.

Caudosacral or caudal vertebrae: Postsacral vertebrae (MLU.GeoS.4077, 4081; Fig. 2k–o, r) bear unicipital, cylindrical transverse processes. The haemal arch is not preserved on either specimen. The spinal nerve foramen is visible posterior to the transverse process and dorsal to the nutritive foramen perforating the transverse process (Fig. 2p, r). There are no foramina anterior to the transverse processes. The ventral lamina is small and inclined, following the inclined foramen for a blood vessel. The transverse process does not extend ventrally from the ventral lamina. The anterior end of the extremely low neural crest starts at the midlength of the vertebra. The neural spine is forked and bears two small spines having blunt ends that were finished with cartilage (Fig. 2r). The foramina ventral to the neural spine are present in MLU.GeoS.4077, whereas in MLU.GeoS.4081, the posterodorsal part of the vertebra is missing.

Atlas: The atlas (Fig. 2v–z') is robust and thick, almost equidimensional (8 mm length x 8 mm width x 7 mm height). The anterior cotyles are shallowly concave, bearing an articulation surface that extends without interruptions across the ventral surface of the odontoid process (Fig. 2y''). The odontoid process lacks a neck. The dorsolateral corners of the odontoid process arise in line with the dorsal edge of the anterior cotyles (Fig. 2y'). In anterior view, the odontoid process follows the cylindrical shape of the floor of the vertebral canal ventrally, and the ventral surface of the process almost reaches the depth of the ventral edge of the anterior cotyles. The odontoid process is only moderately extended anteriorly, but it is wider than either of the anterior cotyles. The anterior and posterior cotyles have circular outlines. No basapophyses, keel, or alar processes are present on the ventral surface. In ventral view, the anterior articulation surface (Fig. 2y'') is anteroposteriorly longest at the mid-width of the odontoid process (Fig. 2w, w'). The dorsal half of the atlas is deformed and laterally shifted to the right. However, the morphology is clearly visible, with a thick and high neural crest (almost as high as the vertebral canal), starting from the anterior edge of the neural arch roof. The dorsal surface of the neural crest is flat and sculptured by several foramina (Fig. 2v, v'). It has a well-defined hourglass shape, slightly more enlarged posteriorly than anteriorly. The postzygapophyses are missing. The foramina for the first spinal nerve are clearly visible posterior to the anterior cotyles (Fig. 2z, z'). Medially in the vertebral canal, the spinal foramen exits anterior to the spinal nerve support (Fig. 2y*).

Remarks and taxonomic comments: The overall morphology of the presacral vertebrae of *Wolterstorffiella* possesses a set of highly plesiomorphic features for caudates, with a unique combination of characters that allows the identification of the species, but no apomorphies of any derived family can be found. The vertebrae share several characters (e.g. the general morphology and proportion of the centrum and the neural canal, the shape of neural crest and spine) with Hynobiidae and North American *Ambystoma* (Ambystomatidae), *Dicamptodon* (Dicamptodontidae) and *Rhyacotriton* (Rhyacotritonidae), a resemblance already noticed by Herre (1950) and Estes (1981). However, all of these groups show a clear set of plesiomorphic features (Estes 1981; Jia et al. 2021) that should not be used for attribution at the family level (e.g. amphicoely). On the contrary, the intravertebral exit (in pre- and/or postsacral vertebrae) of the spinal nerve is considered to be a character typical of derived Salamandroidea (Edwards 1976; Estes 1981). These foramina are clearly visible in both postsacral vertebrae of *Wolterstorffiella* and in most of the presacral vertebrae (Fig. 2p, q). As such, *Wolterstorffiella* can be

placed in Salamandroidea. Attribution to Hynobiidae can be excluded, because hynobiids (and all Cryptobranchoidea) lack spinal nerve foramina in all the postatlantal vertebrae (Edwards 1976). *Ambystoma* shows clear external foramina for the spinal nerves between the presacral vertebrae as well, whereas *Dicamptodon* and *Rhyacotriton* have spinal nerves exiting intervertebrally in the presacral vertebrae and intravertebrally in the postsacral vertebrae (Edwards 1976; Estes 1981).

By the time the material from Walbeck was first described, the above-mentioned North American genera were grouped together in a single family or in a group of closely related families (Herre 1950; Estes 1981). However, recent phylogenetic analyses based on molecular data show *Dicamptodon* and *Ambystoma* to form a clade closely related to Salamandridae, whereas *Rhyacotriton*, together with Amphiumidae and Plethodontidae, are placed in another, second largest clade of salamanders (Pyron and Wiens 2011; Jetz and Pyron 2018). The strong resemblance of their morphology, which led for many years to them being grouped together, is, therefore, the result of shared plesiomorphic characters still retained in the extant taxa. The general proportions between the centrum and neural arch and the reduced presence of zygapophyseal and ventral crests, together with the absence of subcentral keel and basapophyses, exclude attributing *Wolterstorffiella* to Batrachosauroididae and Scapherpetontidae.

The previously unreported, well-preserved atlas (MLU. GeoS.4069) is herein attributed to *Wolterstorffiella wiggeri* based on its morphological similarities with the atlantes of *Ambystoma*, *Dicamptodon* and *Rhyacotriton* and because of an evident size segregation in the salamander specimens from Walbeck, in which vertebrae of *Wolterstorffiella* are the largest (Fig. 3, Table 1). In derived groups of Salamandroidea, the anteroposterior length of the atlas centrum is rather short compared to that of the above-mentioned North American genera, and accounts for at least one-third of the total atlas length formed by the anteriorly projecting odontoid process. A similar long and thick atlas centrum is encountered in *Wolterstorffiella*, and also in the Cretaceous salamandroid *Balveherpeton* (Skutschas et al. 2020; Macaluso et al. 2022b). The extinct families Batrachosauroididae (including the European *Palaeoproteus*) and Scapherpetontidae display anteroposteriorly relatively shorter atlantes. The odontoid process of *Wolterstorffiella* is anteroposteriorly relatively shorter and more primitive compared to the above-mentioned extant North American genera, given its unseparated articulation surface that runs from one cotyle to the other across the ventral surface of the odontoid process. A similar articulation surface is also visible in *Balveherpeton*, pointing again to the basal placement of *Wolterstorffiella* within Salamandroidea. Finally, the neural crest of the atlas in derived groups of Salamandroidea is much lower compared to the atlas here attributed to *Wolterstorffiella* (e.g. Ratnikov and Litvinchuk 2009; Macaluso et al. 2023). The neural crest of *Wolterstorffiella* is comparable in height and thickness to some of the extinct Batrachosauroididae and the above-mentioned extant North American genera. The dorsal sculpturing of the neural crest seen in *Wolterstorffiella* is not present in any of these extant genera or extinct families. However, a similar pattern and extent of ornamentation is visible on atlases or vertebrae of many salamandrid lineages: the Asian salamander/

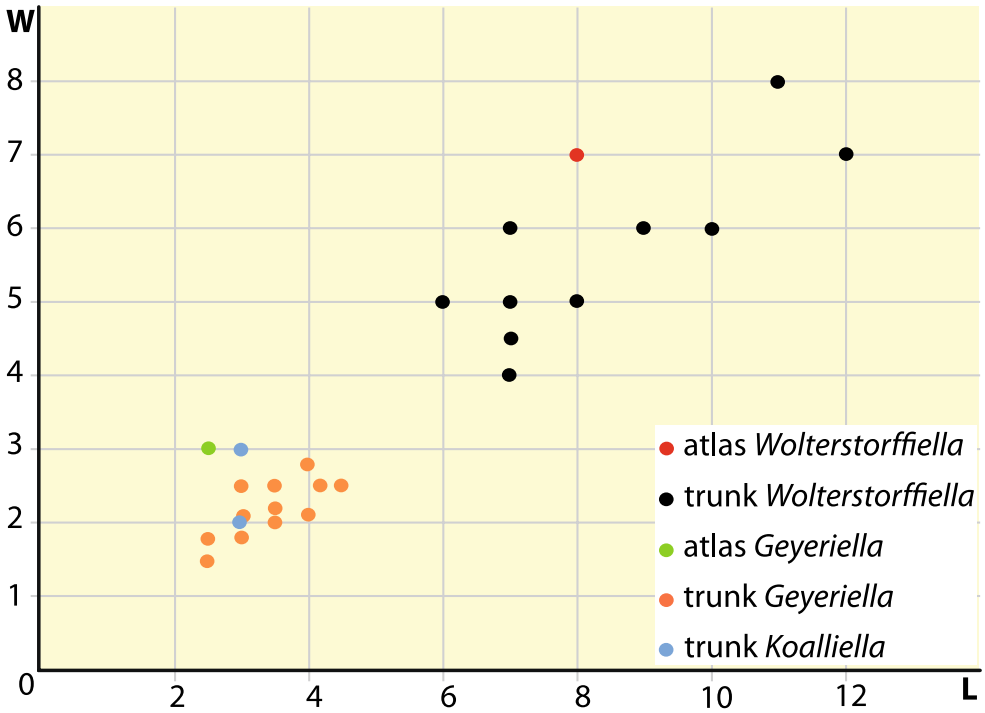

Fig. 3 Size distribution of the three species of Walbeck salamanders according to the length (x-axis) and width (y-axis) of the vertebrae (in mm). Measurements are reported in Table 1

newt genera *Cynops*, *Echinotriton*, and *Tylototriton* (Vasilyan et al. 2017), in some specimens of *Lissotriton helveticus* (see Macaluso et al. 2023), and in extinct *Chelotriton* spp. (Ivanov 2008) and *Lissotriton roehrsi* (Venczel and Hír 2013). The dorsal ornamentation might therefore be plesiomorphic for Salamandroidea (or a subclade, depending on the exact phylogenetic position of *Wolterstorffiella,* which is difficult to assess based on only disarticulated vertebrae) or may have evolved independently at least two times during the evolution of this group. In conclusion, the mosaic of features that can be found in *Wolterstorffiella*, *Dicamptodon*, *Rhyacotriton,* and Salamandridae suggests a placement of *Wolterstorffiella* within Salamandroidea.

Proteidae Bonaparte, 1831
Geyeriella Herre, 1950

Geyeriella mertensi Herre, 1950
(Fig. 4)

Emended diagnosis: Atlas slightly wider than long, possessing a well-developed odontoid process characterised by an unseparated anterior articular surface, and a ventrally projecting wide ventral alar processes. Elongate trunk vertebrae having both amphicoelous and opisthocoelous centra with combination of: dorsoventrally compressed vertebral canal that is lower than the cotyle; long but narrow foramen for blood vessels at the base of parapophyses; bicipital transverse processes with appressed diapophyses and parapophyses; ventral lamina well-developed and trapezoidal in ventral outline; anterior basapophyses present; subcentral keel generally present and variably developed.
Apomorphies: Three characters based on the matrix of Skutschas et al. (2024): ventral fossa at the base of the odontoid process (ch. 16); anterior basapophyses on the trunk vertebrae (ch. 20); and transverse processes are bicipitate and appressed (ch. 24)
Lectotype (lost): The original description of Herre (1950) did not designate a holotype. Later, Estes (1981: p. 48) designated one figured trunk vertebra of Herre (1950: fig. 7) as a lectotype and stated that the specimen was lost. We could not relocate this vertebra in the collection of the MLU, where all the Walbeck material is housed; thus, below we designate a neotype from Herre's (1950) surviving type series.
Neotype: trunk vertebra, MLU.GeoS.4007 (Herre 1950: fig. 11; Fig. 4a–e').
Paralectotypes: Thirteen trunk vertebrae: MLU.GeoS.4000, MLU.GeoS.4001 (Fig. 4i, i'), MLU.GeoS.4004, MLU.GeoS.4005, MLU.GeoS.4007 (Herre 1950: fig. 11; Fig. 4r), MLU.GeoS.4008, MLU.GeoS.4009 (Fig. 4h), MLU.GeoS.4010 (Herre 1950: fig. 12), MLU.GeoS.4013 (Fig. 4g), MLU.GeoS.4015, MLU.GeoS.4016, MLU.GeoS.4019, MLU.GeoS.4031. One possible sacral, MLU.GeoS.4002 (Fig. 4p, q). Two possible caudosacrals: MLU.GeoS.4006 (Herre 1950: fig. 10; Fig. 4j), MLU.GeoS.4023 (Herre 1950: fig. 8; Fig. 4f, s). Two caudal vertebrae: MLU.GeoS.4011 (Fig. 4k–o), MLU.GeoS.4012 (Herre 1950: fig. 9).
Referred material: One atlas, MLU.GeoS.4018 (Fig. 4t–z), described as part of the type series of *Koalliella genzeli* by Herre (1950: fig. 13), see "Remarks" for *Geyeriella* and *Koalliella*.

Description and remarks

Trunk vertebrae: The description is based on the neotype specimen if not otherwise specified. The trunk vertebrae (and the postsacral vertebrae as well) are rather elongate (average L\W ratio: 2:1) with centra lengths of 2.5–4.5 mm (Table 1). Centra are variably amphicoelous (MLU.GeoS.4010, 4013, 4019, 4015, 4023), semiopisthocoelous (i.e. with the inner walls thickly lined with calcified cartilage, but with the notochordal foramen still visible, see Denton and O'Neill 1998: MLU.GeoS.4007, 4009, 4016) or opisthocoelous (note that we follow the "opisthocoely" definition of Auffenberg (1961) and Wake (1966)). In the opisthocoelous condition, the notochordal foramen is not visible in anterior view. The anterior condyle varies from a deep concavity (Fig. 4f, g) (MLU.GeoS.4002) to a shallow concavity (Fig. 4h) (MLU.GeoS.4000, 4005, 4006, 4008) or instead is strongly convex (Fig. 4i, i', j) (MLU.GeoS.4001, 4004, 4031). The anterior condyle consistently lacks a neck. The centrum is relatively laterally compressed in some specimens; it is higher and wider than the vertebral canal, which is strongly to slightly dorsoventrally compressed and pentagonal.

In trunk vertebrae, the nutritive foramen at the base of the parapophyses is generally not wide, but is long (Fig. 4e). The trapezoidal ventral lamina is formed by the ventral surface of the parapophyses and by two small anterior ventral crests (Fig. 4b').

The transverse processes are formed by hollow, appressed diapophyses and parapophyses that broadly contact each other. The diapophysis seems slightly smaller than the parapophysis. The centrum and lateral walls of the neural arch are generally smooth. The anterior and posterior zygapophyseal crests are absent or only the anterior ones are slightly visible, being weakly developed near the prezygapophyses and disappearing posteriorly before reaching the diapophysis (e.g. MLU.GeoS.4005: Fig. 4e'). Foramina for the spinal nerve do not pierce the neural arch in the trunk vertebrae (Fig. 4p, r).
?Sacral and caudosacral vertebrae: In the caudal vertebrae (MLU.GeoS.4011–12: Fig. 4k–o') and in two vertebrae that do not display a haemal arch (MLU.GeoS.4006, 4023; e.g. Fig. 4s for latter specimen), the foramen for the intravertebral exit of the spinal nerves are clearly visible posterior to the diapophyses. As such, MLU.GeoS.4006 and 4023 are interpreted as caudosacral vertebrae. We infer that the foramina for the spinal nerves are absent in trunk

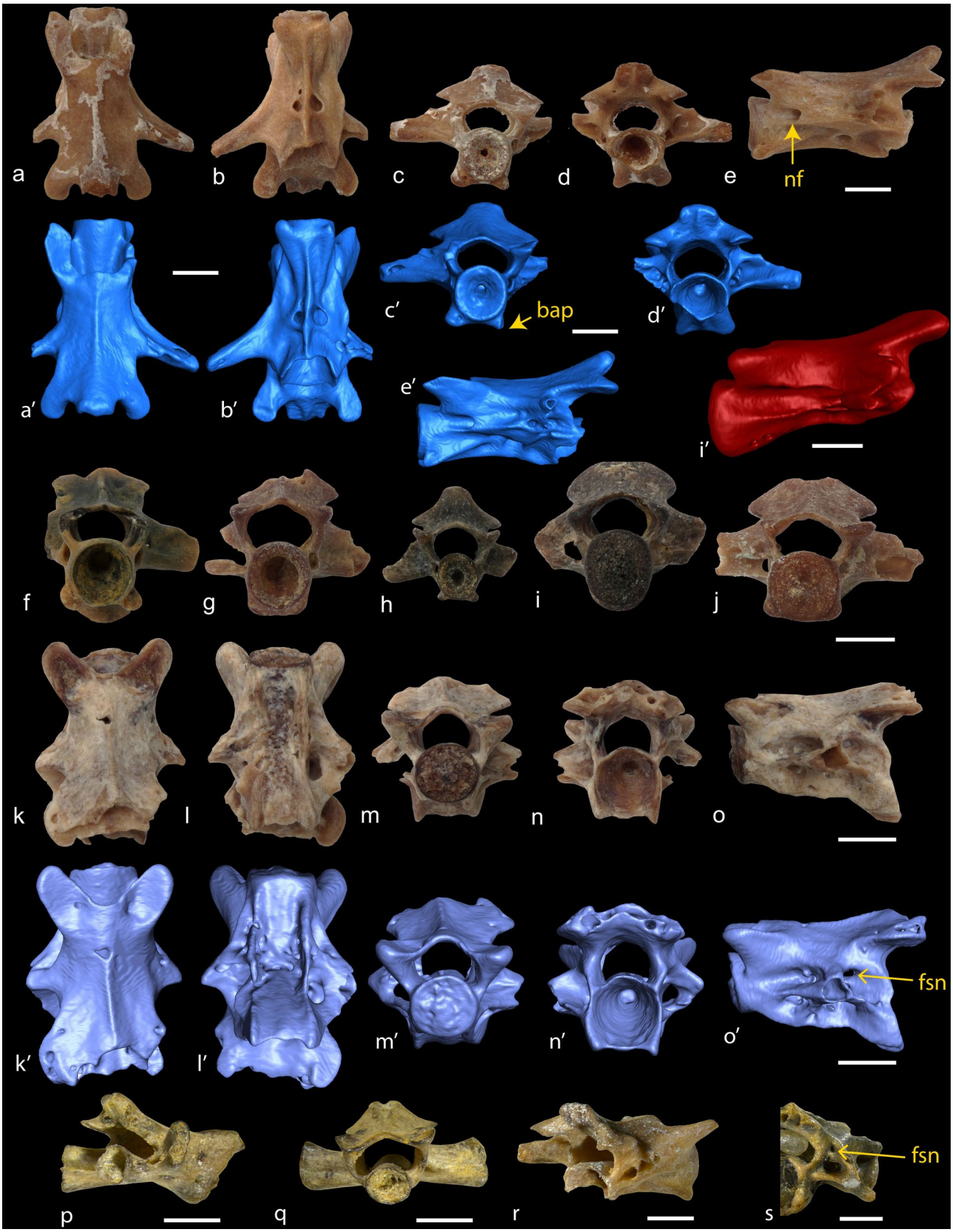
a
b
c
d
e
nf
a′
b′
c′
bap
d′
e′
i′
f
g
h
i
j
k
l
m
n
o
k′
l′
m′
n′
o′
fsn
p
q
r
s
fsn

Fig. 4 Photographs (**a**–**e**, **f**–**o**, **p**–**x**) and 3D-models (**a'**–**e'**, **k'**–**o'**, **t'**–**z'**) of the neotype, selected paralectotypes and referred vertebrae of *Geyeriella mertensi* Herre, 1950 from Walbeck. **a**–**e'** MLU.GeoS.4007 (neotype), trunk vertebra, entire specimen in dorsal (**a**, **a'**), ventral (**b**, **b'**), anterior (**c**, **c'**), posterior (**d**, **d'**) and left lateral (**e**, **e'**) views. **f**–**j** trunk vertebrae in anterior view showing variable condition of filling of the anterior cotyle: **f** MLU.GeoS.4023 (paralectotype), amphicoelous trunk vertebra; **g** MLU.GeoS.4013 (paralectotype), amphicoelous trunk vertebra; **h** MLU.GeoS.4009 (paralectotype), partially opisthocoelous trunk vertebra; **i**, **i'** MLU.GeoS.4001 (paralectotype), opisthocoelous trunk vertebra in anterior (**i**) and left lateral (**i'**) views; **j** MLU.GeoS.4006 (paralectotype), opisthocoelous trunk vertebra. **k**–**o'** MLU.GeoS.4011 (paralectotype), caudal vertebra, entire specimen in dorsal (**k**, **k'**), ventral (**l**, **l'**), anterior (**m**, **m'**), posterior (**n**, **n'**), and left lateral (**o**, **o'**) views. **p**–**s** close-ups of postatlantal vertebrae showing variable condition of spinal nerve foramina: **p**, **q** MLU.GeoS.4002 (paralectotype), sacral vertebra in right posterolateral (**p**) and anterior (**q**) views, lacking spinal nerve foramen; **r**, MLU.GeoS.4007 (paralectotype), trunk vertebra in right posterolateral view, lacking spinal nerve foramen; **s**, MLU.GeoS.4023 (paralectotype), possible caudosacral vertebra in right posterolateral view, showing large spinal nerve foramen; a spinal nerve foramen also occurs on the left side. **t**–**z** MLU.GeoS.4018 (referred), atlas, entire specimen in dorsal (**t**, **t'**), ventral (**u**, **u'**), anterior (**v**, **v'**), posterior (**w**, **w'**), left lateral (**x**, **x'**), left posterolateral (**y**), and anterolateral (**z**) views, and digitally sectioned sagittally (**x''**) to show spinal foramen and spinal nerve support in medial surface of right side; black dashed line (**z**) indicates margins of the anterior articular surface on the left anterior cotyle and onto adjacent portion of the odontoid process. Abbreviations: *aas* anterior articular surface; *ac* anterior cotyle; *bap* basapophysis; *da* dorsal alar process; *fsn* foramen for spinal nerve; *ica* incisura vertebralis caudalis; *icr* incisura vertebralis cranialis; *nf* nutritive foramen; *op* odontoid process; *pc* posterior cotyle; *sns* spinal nerve support; *va* ventral alar process; *vc* vertebral canal; *vf* ventral foramen; *vfs* ventral fossa. Specimens at different magnifications; see corresponding 1 mm scale bars

vertebrae and present in postsacral vertebrae. Corroborating the hypothesis that these specimens are caudosacral vertebrae, the latter specimens are the only vertebrae possessing small posterior basapophyses, as is typical for second or third caudosacral vertebrae of Salamandridae (Macaluso et al. 2023). MLU.GeoS.4002 (Fig. 4p–q) is probably a sacral vertebra, as shown by the low neural crest and spine and by the thick and long transverse processes, which also are not hollow (which presumably makes them stronger). In this specimen, the foramen for the spinal nerve is absent, but the posterior edge of the neural arch is indented, similar to what is observed in the Early Cretaceous *Galverpeton ibericum* (Estes and Sanchíz 1982a: fig. 6). The prezygapophyses are dorsally concave and elliptic. The anterior cotyle or condyle is visible in dorsal view through the anteromedial notch of the neural arch. In dorsal view, the vertebra is not hourglass-shaped, but sub-rectangular, with a rather cylindrical shape. The neural crest is low and barely reaches the base of the neural spine. The neural spine is forked or forms a single bulge, almost reaching the posterior edge of the postzygapophyses. In posterior view, the neural arch and neural spine are rather flat, and not dorsally pointed. In the trunk vertebrae, the anterior basapophyses are generally present, except for specimens MLU.GeoS.4001 and MLU.GeoS.4010, where their condition is uncertain because of the preservation of the vertebrae. The subcentral keel can be present and variably developed, or rarely absent. In particular, two vertebrae have an extremely shallow subcentral keel (MLU.GeoS.4000 and 4005), and two vertebrae lack a

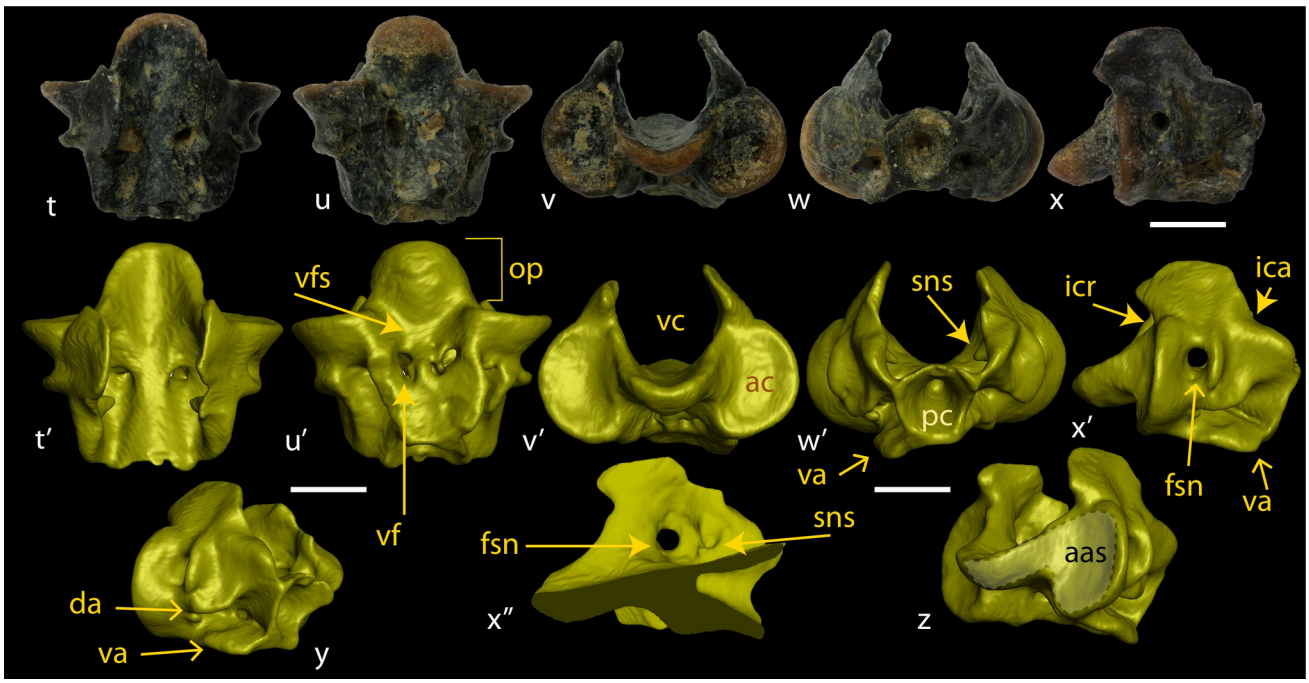

Fig. 4 (continued)

subcentral keel (MLU.GeoS.4004 and 4019). It is possible that a trend of reduced subcentral keel was present along the vertebral column, and thus, these vertebrae are closer to the sacral region (a similar trend to that shown by the late Palaeocene–early Eocene *Seminobatrachus boltyschkensis*: Skutschas and Gubin 2012). In the sacral vertebra (MLU.GeoS.4002), both basapophyses and subcentral keel are absent (Fig. 4p, q). In the caudosacrals, the anterior basapophyses are present, but the subcentral keel is absent.

Caudal vertebrae: The caudal vertebrae bear unicipital and cylindrical transverse processes. The haemal arch is not preserved in either specimen. The spinal nerve foramen is visible posterior to the transverse process and dorsal to the foramen perforating the transverse process (Fig. 4o, o'). Anterior to the transverse processes, one or two foramina are visible. The ventral lamina is wide and posteroventrally inclined, paralleling the inclined foramen for blood vessels. The transverse process is ventrally extruding from the ventral lamina. A cavity is present anterior and posterior to the base of the transverse processes. External surfaces of the centrum and base of the neural arch are highly perforated (Fig. 4l'). In both specimens, the neural spine is broken at its base and the dorsoposterior part of the neural arch.

Atlas: The centrum of the atlas (Fig. 4t–z) is slightly wider than long (width=4 mm; length=3.5 mm). The articular surfaces of the anterior cotyles are flat and slightly mediolaterally compressed. The odontoid process projects anteriorly for a moderate distance and is relatively wide. The ventral margin of the odontoid process is located above the ventral margin of the cotyles (Fig. 4v'). In ventral view, a ventral fossa is present at the base of the odontoid process (Fig. 4u'). This ventral fossa continues anterolaterally as two grooves that end lateral to the base of the odontoid process articular surface. The ventral fossa at the base of the odontoid process is flanked by two well-developed ventral and dorsal alar processes, each originating anteriorly from the medial side of the anterior cotyles (Fig. u'). These crest-like processes extend posteroventrally to the posterior edge of the cotyle. The ventral surface of the centrum between the alar processes is concave and bears a couple of symmetrical ventral foramina that perforate the ventral wall of the vertebral canal (Fig. 4u, u'). Dorsal to the ventral alar processes, there is a deep groove delimited by the ventral alar process ventrally and by the dorsal alar process dorsally (Fig. 4y). Internal to this groove and posterior to the anterior cotyles, there is a pair of lateral foramina per each side (Fig. 4y). On each lateral side of the neural arch, a lateral crest posteriorly borders the large foramen for the first spinal nerve (Fig. 4x'). Medially in the wall of the vertebral canal, the spinal nerve foramen is located anterior to the spinal nerve support (Fig. 4x''). The roof of the neural arch is broken, but on both sides, the deep incisurae caudalis and cranialis are visible.

Remarks and taxonomic comments: The atlas MLU.GeoS.4018 was originally part of the type series of the salamandrid *Koalliella genzeli* Herre, 1950 and accepted as such by Estes (1981), but based on the morphology of the odontoid process and the alar processes of the atlas, an attribution to Salamandridae can be excluded. This specimen is herein attributed to *Geyeriella mertensi* due to its close similarity with the atlas attributed to the younger (Miocene) *Geyeriella wettsteini* (originally as *Bargmannia wettsteini*, Herre 1955; see Estes 1981 and Macaluso et al. 2022b for the synonymization of *Geyeriella* and *Bargmannia*). *G. mertensi* was stated to differ from *G. wettsteini* based on its transverse processes having a larger separation between the diapophyses and parapophyses (Herre 1955). Appressed diapophyses and parapophyses are consistently seen in all trunk vertebrae of *G. mertensi* and clearly differ from the condition figured by Herre (1955) for *G. wettsteini*; that difference supports recognising them as different species within *Geyeriella*.

The caudal vertebrae of *Geyeriella mertensi* can be differentiated from the ones of the co-occurring *Wolterstorffiella wiggeri* because they are considerably smaller (Fig. 3, Table 1), they have either a partially opisthocoelous centrum (MLU.GeoS.4011) or some osseous depositions on the inner walls of the anterior cotyle (MLU.GeoS.4012), and have a better developed ventral lamina anterior and posterior to the unicipital transverse process.

The vertebrae of both species of *Geyeriella* share common features with *Seminobatrachus boltyschkensis* from the late Palaeocene–early Eocene of Ukraine (Skutschas and Gubin 2012). The latter species is known from articulated specimens that show a similar morphology of basapophyses and subcentral keel as those herein reported for *Geyeriella mertensi*: the anterior basapophyses are consistently present on the trunk vertebrae, and the subcentral keel becomes shallower towards the sacral vertebra. The detailed morphology of the atlas and the sacral vertebrae of *S. boltyschkensis* are unknown (Skutschas and Gubin 2012). However, the Ukrainian species is described as consistently bearing the spinal nerve foramen in all trunk vertebrae. Skutschas and Gubin (2012: p. 144) stated that "the spinal nerve foramen is visible on the inner surface of the base of the neural arch", but in figure 2C in Skutschas and Gubin (2012) the foramen seems to be visible on the external surface as well, which would be sufficient to retain these taxa as separate genera. Further studies on *S. boltyschkensis* are pending, and the species should, therefore, be considered a valid Palaeogene species of salamander. Nevertheless, a close relationship between these genera can be suggested. In many respects, including the shape of the ventral alar process and the shape of the odontoid process, the atlas of *G. mertensi* is similar to the atlas of *Apricosiren* (from the Early Cretaceous of UK; Evans and McGowan 2002), however it can be differentiated by having the centrum slightly wider than long (vs. the opposite for *Apricosiren*). The pattern of intra-/intervertebral exit of the spinal nerves is also shared with the UK taxon, but *Geyeriella* can be differentiated from it because

Geyeriella lacks posterior basapophyses and typically has a subcentral keel.

The attribution of *Geyeriella mertensi* to stem-urodeles and Cryptobranchoidea can be excluded by the presence of the spinal nerve foramina, respectively, in the atlas and in the postsacral vertebrae. Many features displayed by *Geyeriella* evolved several times in different salamandroid groups. For example, the subcentral keel is present in extant Proteidae, Sirenidae and Amphiumidae, and in the extinct Batrachosauroididae and Scapherpetontidae. The anterior basapophyses are visible in the extant Sirenidae, Amphiumidae and the genus *Ambystoma* (in all the presacral vertebrae, atlas included) and in the extinct Batrachosauroididae. However, the trunk vertebrae of *G. mertensi* differ from those of Sirenidae in having bicipital transverse processes and lacking both the 'Y'-shaped configuration of the neural crest and spinal nerve foramina. The small anterior ventral crests strongly differ from the wide anterior alar process (Gardner 2003a, b) of Amphiumidae and Sirenidae. *Geyeriella* further differs from the Amphiumidae in having an unseparated articular surface of the odontoid process of the atlas. Both the atlas and post-atlantal vertebrae of *G. mertensi* can be clearly distinguished from the Batrachosauroididae and Scapherpetontidae in being considerably less robust and more elongated, with wider vertebral canals. Moreover, the anterior cotyles of the atlas are shallower, the odontoid process is wider, and a wide ventral alar process is present on its ventral surface. In all these respects, both the atlas and other vertebrae resemble closely the extinct proteid *Paranecturus garbani* from the late Maastrichtian of North America (DeMar 2013).

The atlas of *Geyeriella mertensi* resembles *Paranecturus garbani* and differs from most other proteids (except *Euronecturus grogu*) in having a wider odontoid process, with an extensive articular surface. The atlas differs from *E. grogu* in the more concave and equidimensional anterior cotyles, but resembles *E. grogu* in having a ventral fossa at the base of the odontoid process. The trunk vertebrae bear an unicipitate neural spine and bicipital transverse processes similar to *Necturus maculosus* and *N. krausei* (vs. neural spine forked and unicipital transverse processes in *Mioproteus* and *Proteus*). In *N. krausei* and *G. mertensi* the diapophysis is hollow (vs. other proteids have solid diapophyses). *Geyeriella* differs further from *Mioproteus* in the absence of posterior basapophyses.

Geyeriella differs from other proteids in having caudosacral and caudal vertebrae pierced by spinal foramina (condition unknown for *Paranecturus*) and in having opisthocoelous centra bearing anterior basapophyses. Opisthocoely is generally considered a derived feature among caudatans; i.e. extant Salamandridae and Plethodontidae, and extinct Batrachosauroididae. Salamandrids show a different pattern of calcification infilling compared to the one observed in *Geyeriella*, the latter of which is more similar to the pattern in Plethodontidae and Batrachosauroididae (Estes and Sanchíz 1982a). Moreover, salamandrids tend to be consistently opisthocoelous, with transitional stages rarely or never reported (Ratnikov and Litvinchuk 2007; Macaluso et al. 2023). On the contrary, Wake (1966) stated that in the plethodontid *Thorius* group of genera, transitional stages (like the ones observed in *Geyeriella*) between amphicoely and opisthocoely often occur. An opisthocoelous condition or transitional stages with a certain degree of ossification have never been reported in proteids. However, because all extant proteids are obligate paedomorphic species, one cannot exclude that some sort of calcification of the anterior cotyle could have occurred in extinct proteids (similar to what is observed in plethodontids and in the extinct batrachosauroidids).

Salamandridae Goldfuss, 1820
Koalliella Herre, 1950

Koalliella genzeli Herre, 1950
(Fig. 5)

Emended diagnosis: Trunk vertebrae with the combination of: thick wall of the neural arch between the anterior ventral crests and the prezygapophyses, perforated by the nutritive foramen; high neural crest, posteriorly enlarging, and slightly thickened dorsally by the presence of a small dermal capsule (smooth and slightly concave, but not pitted); neural crest in posterior view forming a wide, flat horizontal surface with lateral margins that are relatively straight and not wavy.
Apomorphies: Six characters based on the matrix of Macaluso et al. (2023) (note that using the matrix of Skutschas et al. 2024, no apomorphies could be found): the lateral lips of the neural crest of the precaudal vertebrae are present (1) (ch. 50); in ventral view, the ventral lamina of the precaudal vertebrae has symmetrically rhomboidal shape (ch. 67); in anterior view, the basal portion of the walls of the neural arch of the caudal vertebrae starts more laterally than the haemal arch (ch. 72); the transverse processes of the caudal vertebrae in lateral view in the anterior half of the tail is horizontal, with three parallel laminae (zygapophyseal, middle, ventral crests) (ch. 75); the height/length ratio of the caudal vertebrae varies between 1.25 and 1.4 (ch. 76); in lateral view, the anterior margin of the haemal arch ventrally to the anterior ventral crest is concave or posteriorly inclined (ch. 81)

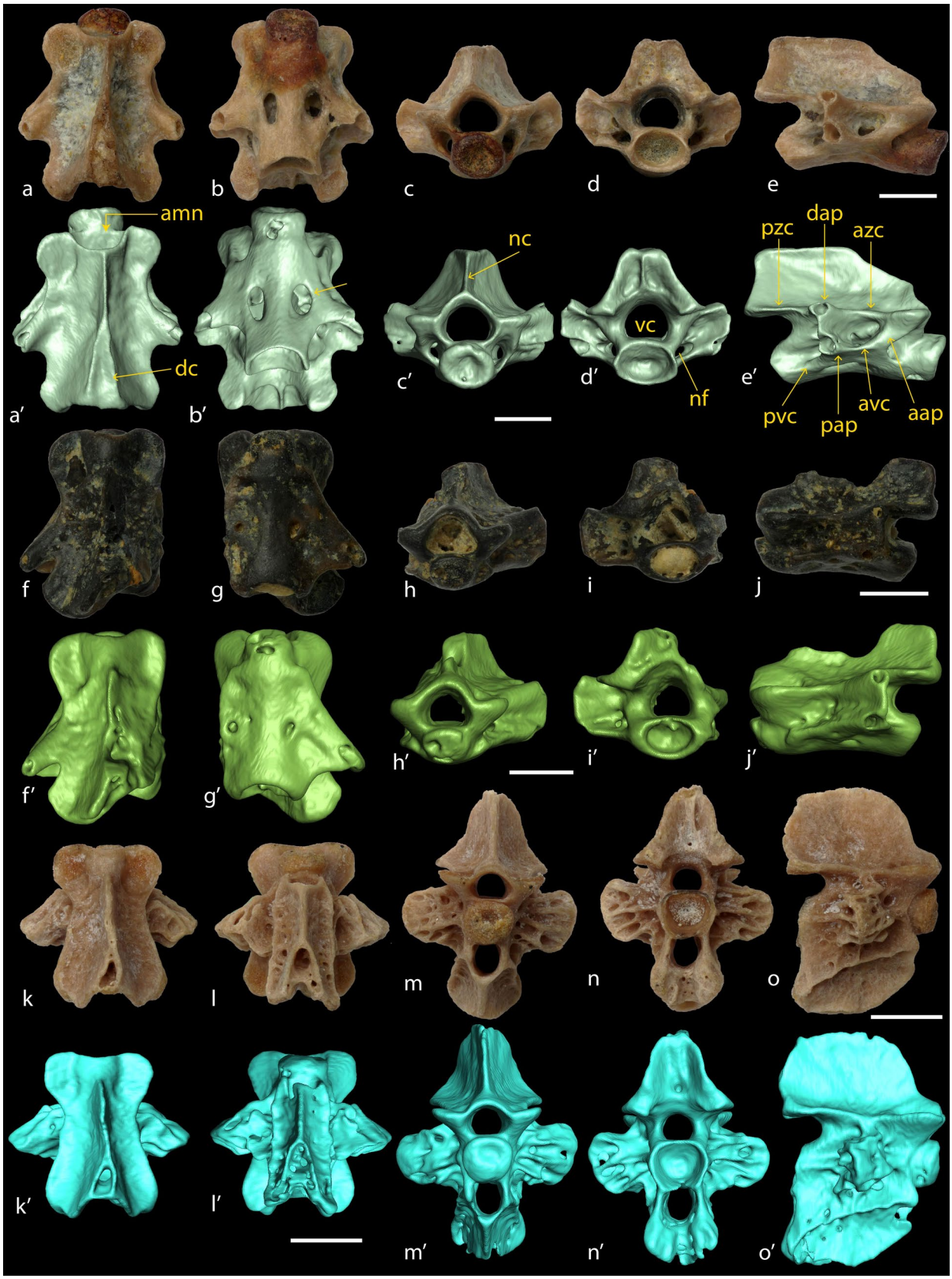
a
b
c
d
e
amn
dc
a′
b′
nc
c′
vc
d′
nf
pzc
dap
azc
e′
pvc
pap
avc
aap
f
g
h
i
j
f′
g′
h′
i′
j′
k
l
m
n
o
k′
l′
m′
n′
o′

◂**Fig. 5** Photographs (**a–e**, **f–j**, **k–o**) and 3D-models (**a'–e'**, **f'–j'**, **k'–o'**) of the lectotype and paralectotypes of *Koalliella genzeli* Herre, 1950 from Walbeck. **a–e'** MLU.GeoS.4017 (lectotype), trunk vertebra, entire specimen in dorsal (**a**, **a'**), ventral (**b**, **b'**), anterior (**c**, **c'**), posterior (**d**, **d'**), and right lateral (**e**, **e'**) views. **f–j'**, MLU.GeoS.4003 (paralectotype), trunk vertebra, entire specimen in dorsal (**f**, **f'**), ventral (**g**, **g'**), anterior (**h**, **h'**), posterior (**i**, **i'**), and left lateral (**j**, **j'**) views. **k–o'**, MLU.GeoS.4014 (paralectotype), caudal vertebra, entire specimen in dorsal (**k**, **k'**), ventral (**l**, **l'**), anterior (**m**, **m'**), posterior (**n**, **n'**), and lateral (**o**, **o'**) views. Abbreviations: *aap* accessory alar process; *amn* anteromedial notch; *avc* anterior ventral crest; *azc* anterior zygapophyseal crest; *dap* diapophysis; *dc* dermal capsule; *nc* neural crest; *nf* nutritive foramen; *pap* parapophysis; *pvc* posterior ventral crest; *pzc* posterior zygapophyseal crest; *sf* subcentral foramen; *vc* vertebral canal. Specimens at different magnifications; see corresponding 1 mm scale bars

Lectotype: One trunk vertebra, MLU.GeoS.4017 (Herre 1950: fig. 15; Fig. 5a–e'). Previously designated without an institutional specimen number by Estes (1981: p. 81).
Paralectotypes: One trunk vertebra, MLU.GeoS.4003 (Herre 1950: fig. 14; Fig. 5f–j'), and one caudal vertebra, MLU.GeoS.4014 (Herre 1950: fig. 16; Fig. 5k–o').

Description and remarks

Trunk vertebrae: Our description of the trunk vertebrae is based mostly on the lectotype (Fig. 5a–e'), because it is better preserved than the paralectotype (Fig. 5f–j'). The trunk vertebrae are opisthocoelous, and the notochordal foramen is not present. The anterior condyle has a poorly-pronounced neck and a round outline (Fig. 5b', g'). The vertebral canal has a pentagonal outline. The posterior cotyle is slightly dorsoventrally compressed (Fig. 5d', i').

The lectotype (MLU.GeoS.4017) measures 3 mm in both length and width. The nutritive foramen at the base of the parapophyses is wide. The wide anterior ventral crests are nearly horizontal (Fig. 5e, j), forming the anterior part of the ventral lamina. An additional crest (accessory alar process sensu Vasilyan et al. 2017) connects the anterior ventral crest and the prezygapophysis and is medially perforated by the nutritive foramen (Fig. 5e, e'). In MLU.GeoS.4003, the accessory alar process is absent on the left, and possibly not preserved on the right (Fig. 5j).

The ventral lamina is perforated by two long subcentral foramina flanking the vertebral centrum in MLU.GeoS.4017. In MLU.GeoS.4003, the lamina is rhomboidal in shape, and the two foramina are smaller than in MLU.GeoS.4017. The posterior ventral crests are small, appressed to the transverse processes (Fig. 5e'). The transverse processes are formed by hollow diapophyses and parapophyses that do not contact each other, but are connected by a lamina. The dorsolaterally directed diapophysis is slightly smaller than the parapophysis. The anterior and posterior zygapophyseal crests are well developed, giving the vertebra a rather rectangular shape in dorsal view. The spinal nerve foramina are present posterior to the transverse processes and dorsal to the nutritive foramen.

The prezygapophyses are subhorizontal and have circular to elliptic outlines. They lie in a horizontal plane at half the height of the vertebral canal. The anterior condyle is visible in dorsal view through the anteromedial notch of the neural arch. The neural arch connects the prezygapophyses from their anteromedial edge. The neural crest arises anteriorly at the anterior edge of the neural arch (MLU.GeoS.4017: Fig. 5a') or slightly posterior to it (MLU.GeoS.4003: Fig. 5f'). The neural crest rises steeply and reaches its maximum height anterior to the midlength of the vertebra. The neural crest forms one-third to one-fourth of the total height of the vertebra. The presence of a small dermal capsule dorsally slightly enlarges the neural crest (Fig. 5a'). The dorsal surface of the neural crest enlarges posteriorly, and its dorsal surface is slightly concave, but not pitted (Fig. 5a'). In dorsal view, the posterior cotyle is obscured by the neural arch. In posterior view, there is no incisura dorsalis, and the neural crest forms a flat horizontal surface that is relatively large and with lateral margins that are rather straight and not wavy. The basapophyses and subcentral keel are absent.

Caudal vertebra: The caudal vertebra is opisthocoelous, with high neural and haemal crests (Fig. 5k–o). The morphology of the prezygapophyses and the anteromedial notch of the neural arch are consistent with those of the trunk vertebrae. The spinal nerve foramina pierce the neural arch posterior to the transverse processes. The nutritive foramina are not visible. The transverse processes are present and expanded, formed by four or five sub-horizontal or horizontal laminae separated by grooves and several foramina, but the laminae are clearly fused in the middle to form the laterally extended transverse process (Fig. 5o, o'). The transverse processes are thick in anterior, lateral, and dorsal views, which gives them a rectangular shape. The anterior and posterior ventral crests are connected in a straight line that is ventroposteriorly inclined. The anterior and posterior middle crests are visible anterior and posterior to the transverse processes. The posterodorsal and posteroventral edges of the neural and haemal arches are rounded. In posterior view, the neural crest is proportionally higher than the neural arch compared to the trunk vertebrae, and its dorsal edge is rounded rather than flat. The anterior end of the neural crest arises behind the anterior margin of the neural arch and posteriorly expands to form a triangular shape (Fig. 5m, o). However, the enlarged portion of the crest is much narrower compared to that of the trunk vertebrae. The surface of the neural crest is perforated and not flat as in the trunk vertebrae, even if small lateral eversions (reminiscent of the dermal capsule) seem to be present. The haemal crest is more ventrally enlarged than the neural crest

Table 1 Measurements (in mm) of the salamander vertebrae studied herein from Walbeck. Abbreviations: *H*, height; *L*, length.

Species	Element	coll. nr.	L	H
Wolterstorffiella wiggeri	atlas	4065	8	7
Wolterstorffiella wiggeri	sacral-postsacral vertebra	4070	12	7
Wolterstorffiella wiggeri	trunk vertebra	4071	11	8
Wolterstorffiella wiggeri	trunk vertebra	4072	10	6
Wolterstorffiella wiggeri	trunk vertebra	4073	9	6
Wolterstorffiella wiggeri	trunk vertebra	4074	7	5
Wolterstorffiella wiggeri	trunk vertebra	4075	7	5
Wolterstorffiella wiggeri	trunk vertebra	4076	7	5
Wolterstorffiella wiggeri	caudosacral or caudal vertebra	4077	7	6
Wolterstorffiella wiggeri	trunk vertebra	4078	7	4.5
Wolterstorffiella wiggeri	trunk vertebra	4079	6	5
Wolterstorffiella wiggeri	trunk vertebra	4080	8	5
Wolterstorffiella wiggeri	postsacral vertebra	4081	7	4
Wolterstorffiella wiggeri	trunk vertebra	4082	6	5
Geyeriella mertensi	atlas	4018	4	3.5
Geyeriella mertensi	trunk vertebra	4000	3	2.1
Geyeriella mertensi	trunk vertebra	4001	4.5	2.5
Geyeriella mertensi	?sacral vertebra	4002	3	1.8
Geyeriella mertensi	trunk vertebra	4004	4.5	2.5
Geyeriella mertensi	trunk vertebra	4005	3	2.1
Geyeriella mertensi	?caudosacral vertebra	4006	4.2	2.5
Geyeriella mertensi	trunk vertebra	4007	4	2.1
Geyeriella mertensi	trunk vertebra	4009	2.5	1.8
Geyeriella mertensi	trunk vertebra	4010	3.5	2.5
Geyeriella mertensi	caudal vertebra	4011	3	2.5
Geyeriella mertensi	caudal vertebra	4012	2.5	1.5
Geyeriella mertensi	trunk vertebra	4013	3.5	2.2
Geyeriella mertensi	trunk vertebra	4015	3.5	2
Geyeriella mertensi	trunk vertebra	4016	2.5	1.5
Geyeriella mertensi	trunk vertebra	4019	4	2.1
Geyeriella mertensi	?caudosacral vertebra	4023	4	2.8
Geyeriella mertensi	trunk vertebra	4031	3.5	2.5
Koalliella genzeli	trunk vertebra	4017	3	3
Koalliella genzeli	trunk vertebra	4003	3	2
Koalliella genzeli	caudal vertebra	4014	?	?

and perforated as well. The haemal crest bifurcates slightly past the anteroposterior midpoint of the centrum. The haemal crest starts from the anterior edge of the haemal arch.

Remarks and taxonomic comments: The presence of spinal nerve foramina in both precaudal and caudal vertebrae is only found in derived groups of Salamandroidea (Edwards 1976). As stated earlier, only Plethodontidae, Batrachosauroididae, and Salamandridae evolved an opisthocoelous condition. The aspect of the anterior condyle, particularly its small neck and no notochordal foramen visible, is typical of Salamandridae and is diagnostic for the family (Auffenberg 1961; Ratnikov and Litvinchuk 2007). Moreover, the general morphology of both the caudal and precaudal vertebrae is typical of salamandrids, in having a high neural crest and well-developed zygapophyseal and ventral crests (Ratnikov and Litvinchuk 2007; Macaluso et al. 2023).

Within Salamandridae, the position of *Koalliella genzeli* is uncertain, because the material is inadequate to resolve its phylogenetic position. However, several features of the trunk vertebrae that are shared with different genera of salamandrids point to an early branching position for *K. genzeli* within this group. *K. genzeli* shares with the early branching extant *Salamandrina* the presence of a dermal capsule on the neural crest (Sanchiz 1988; Macaluso et al. 2020), even though in *Koalliella* the dermal capsule seems much less extensive. A dermal capsule is also present in other extant genera of Pleurodelinae (e.g. the Asiatic *Cynops* and the North American *Taricha* and *Nothophtalmus*), including the crocodile newts (e.g. *Tylototriton*) and the closely related extinct *Chelotriton*. Crocodile and ribbed newts share several characters with *Koalliella*. One of these is the presence in some specimens (of both *Pleurodeles* and *Tylototriton*; LM pers.obs.) of the bony connection between the ventral crests and the prezygapophyses, as seen in MLU. GeoS.4017; however, in *Pleurodeles* and *Tylototriton* that bony connection is never perforated by the nutritive foramen as it is in *K. genzeli*. This foramen is not clearly visible in anterior view in *Pleurodeles* and *Tylototriton*, and the presence of a large nutritive foramen is most likely plesiomorphic for urodeles (as shown by the presence of this wide foramen in both hynobiids and stem-salamandroids, together with several more derived taxa; e.g. *Ommatotriton*, see Macaluso et al. 2023). Also, the prezygapophyses laying in a horizontal plane at midheight of the vertebral canal is most likely plesiomorphic, because it is shared with several taxa (e.g. *Pleurodeles*, *Cynops*, *Ambystoma*). The expansion of the ventral lamina is variable, which can be seen in *Salamandra* and *Triturus*. However, the morphology of the rest of the vertebra (e.g. the shape of transverse processes, the height of the neural crest, and the absence of dorsoventrally compressed centrum and/or vertebral canal) is not consistent with these taxa. Finally, the shape of the dorsal edge of the neural crest in posterior view, forming a large and flat horizontal surface with straight lateral margins, is an intermediate state among those shown by the crocodile newts, *Cynops*, *Salamandrina*, and some specimens of *Lissotriton helveticus* (LM pers.obs.). This mosaic of characters points to an early branching position for *K. genzeli* among Salamandridae, however, additional material is needed to assess the phylogenetic position of the species confidently.

Phylogenetic analyses of Walbeck salamanders

To test the phylogenetic position of the Walbeck salamanders, we ran a vertebrae-based phylogenetic analysis using two matrices. The trees were obtained through maximum parsimony analysis. The first analyses, obtained from the vertebrae-based matrix of Skutschas et al. (2024), retained

two trees when *Rhyacotriton* was included (strict consensus tree in Fig. 6a; C.I. 0.493, R.I. 0.681) and only one tree when *Rhyacotriton* (the most unstable taxon in the phylogeny) was excluded (Fig. 6b; C.I. 0.500, R.I. 0.690). The position of the three genera of Walbeck salamanders does not vary: *Geyeriella* is at the base of Proteidae, *Wolterstorffiella* at the base of a clade ("united" clade) of a subset of Salamandroidea taxa, and *Koalliella* is the sister of *Lissotriton helveticus*, the only species of Salamandridae included in the analysis.

To better resolve the phylogenetic position of *Koalliella*, we ran a second analysis, based on the Salamandridae matrix of Macaluso et al. (2023). That analysis retained ten trees, and the strict consensus tree is figured in Figure 6d (C.I. 0.577, R.I. 0.605). The results of our analysis could not reflect the molecular results, being based on morphological

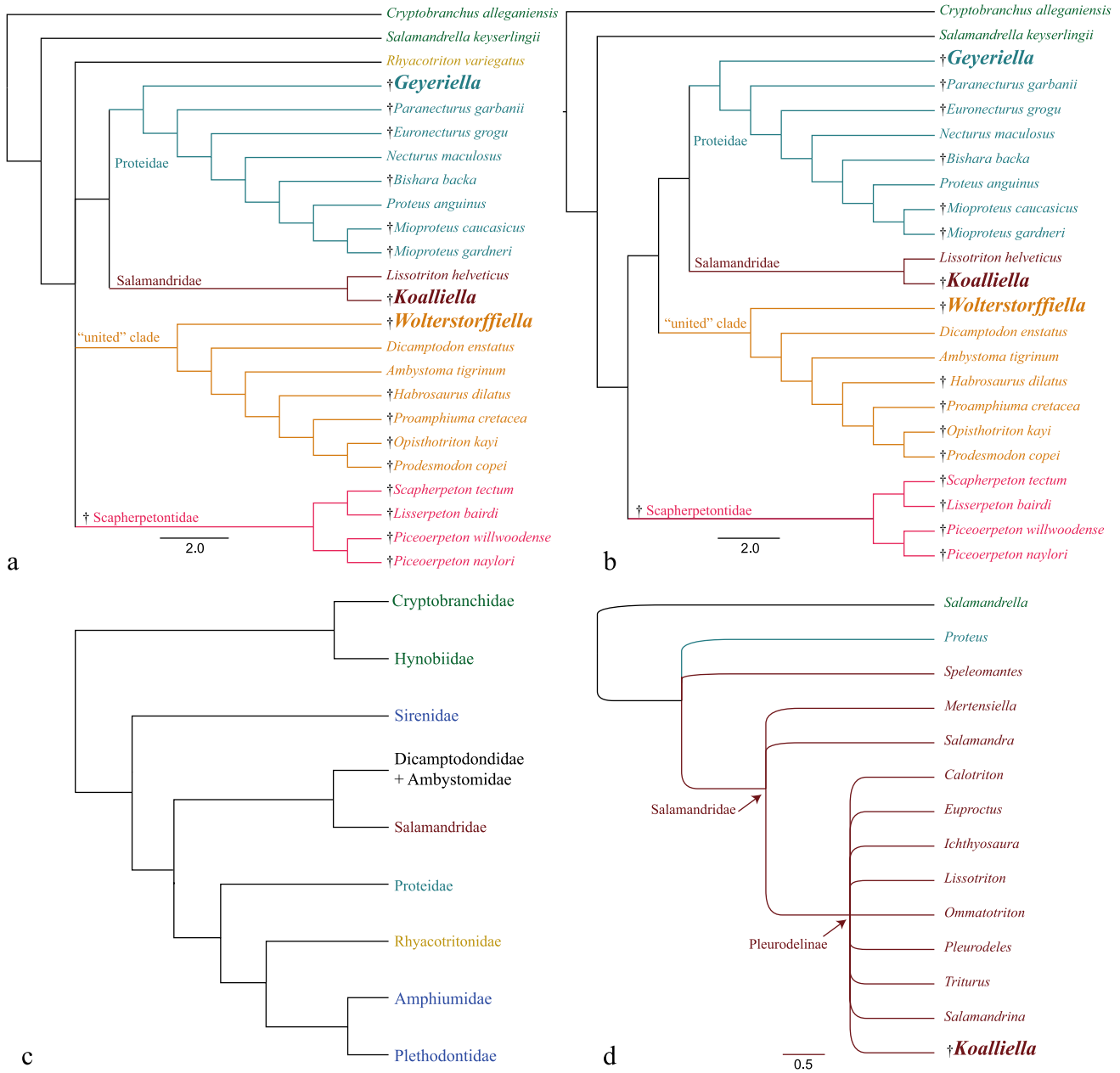

Fig. 6 Phylogenetic trees, including the Walbeck caudate taxa, obtained through maximum parsimony analysis. **a**, **b** Strict consensus trees based on the dataset of Skutschas et al. (2024) with (**a**) and without (**b**) the unstable *Rhyacotriton variegatus*. **c** Phylogenetic tree of recent salamander families after Pyron and Wiens (2011). **d** Strict consensus tree of the main Salamandridae genera based on the dataset of Macaluso et al. (2023). The bar at the bottom provides the scale of branch lengths

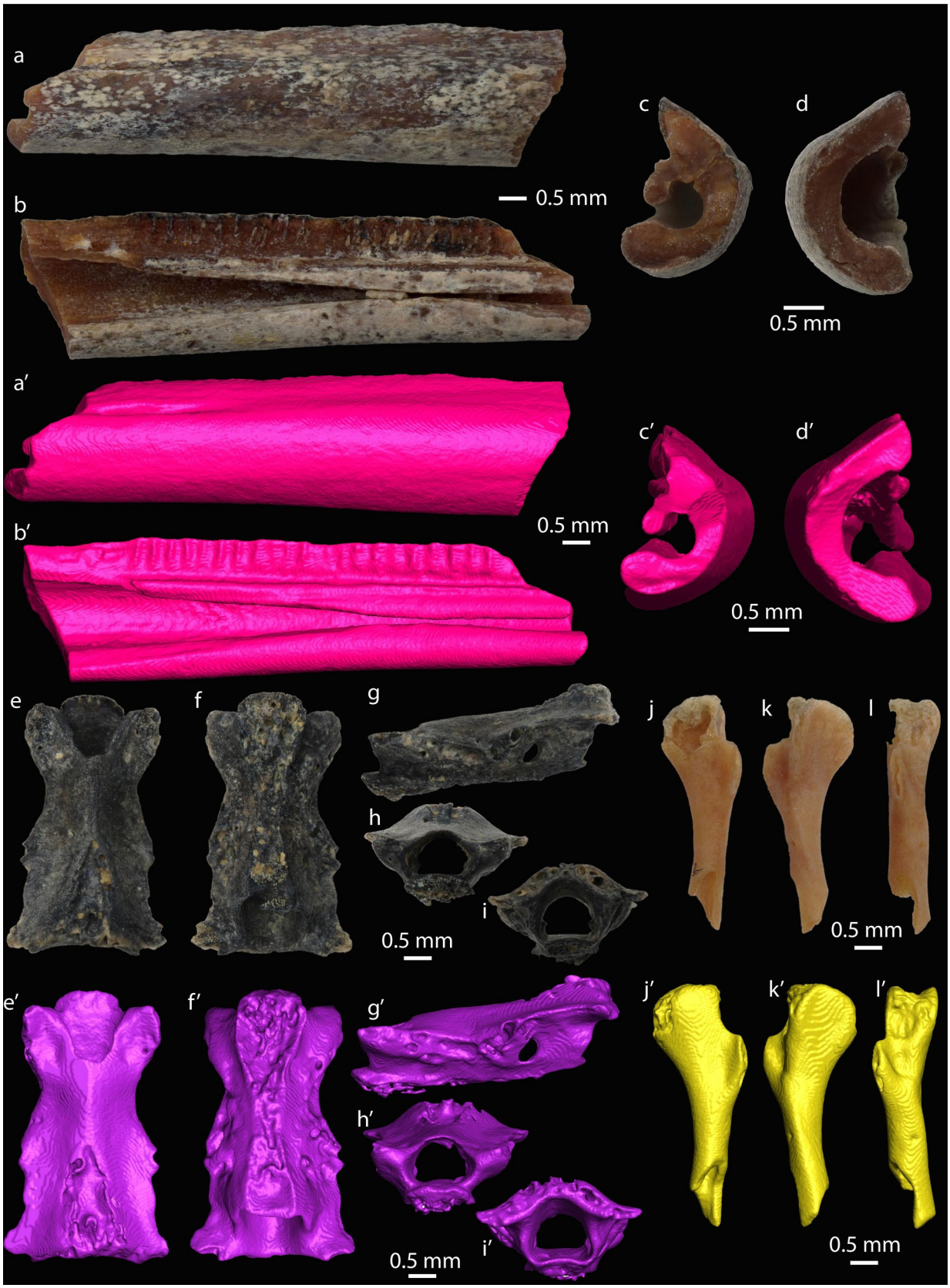
a
b
0.5 mm
c
d
0.5 mm
a′
b′
0.5 mm
c′
d′
0.5 mm
e
f
g
h
i
0.5 mm
j
k
l
0.5 mm
e′
f′
g′
h′
i′
0.5 mm
j′
k′
l′
0.5 mm

◂**Fig. 7.** Bones of Caudata indet. from Walbeck. **a–d'** MLU.GeoS.4028, dentary, entire specimen in labial (**a**, **a'**), lingual (**b**, **b'**), anterior (**c**, **c'**), and posterior (**d**, **d'**) views. **e–i'** MLU.GeoS.4021, fragmentary vertebra, entire specimen in dorsal (**e**, **e'**), ventral (**f**, **f'**), left lateral (**g**, **g'**), anterior (**h**, **h'**), and posterior (**i**, **i'**) views. **j–l'** MLU.GeoS.4020, femur, entire specimen in lateral (**j**, **j'**), mesial (**k**, **k'**), and dorsal (**l**, **l'**) views. Specimens at different magnifications; see corresponding scale bars

data only. Consequently, *Salamandrina* is not recovered as the most early branching genus of Salamandridae, but instead groups in the "Pleurodelinae" clade. *Salamandrina* cannot be separated in our analysis from the true Pleurodelinae (Fig. 6d) because its bone morphology is similar (convergently or plesiomorphically) with that of Pleurodelinae (see e.g. Veith et al. 2018). For the same reason, we also question the position of *Koalliella*, which could equally occupy an early branch within Salamandridae (similar to *Salamandrina*) or, as in our analysis, be nested within Pleurodelinae.

In general, vertebrae morphology is considered less informative for discerning relationships among the families of urodeles, but useful for assigning isolated vertebrae to a family (Naylor 1979). This is reflected in the phylogenetic topologies obtained using the vertebrae-only morphological matrix of urodeles originally from DeMar (2013; latest version of Skutschas et al. 2024). Our analyses based on the latter dataset successfully groups members of the same families together, but the relationship between the clades, i.e. superfamilies and families, remains unclear (as shown by differences compared to the topology based on molecular analyses depicted in Fig. 6c). In our analysis, *Geyeriella* is an early branching Proteidae, sharing with other members of the family the presence of the ventral alar process (= alar-like process sensu Venczel and Codrea (2018)) of the atlas (ch. 10). *Wolterstorffiella* never forms a clade with *Dicampton* and/or *Ambystoma*, and, as such, the similar vertebral morphology is considered to be retained as a plesiomorphic condition in these taxa, and the previous attribution of *Wolterstorffiella* to Dicamptodontidae (Estes 1981) is currently discarded. However, *Wolterstorffiella* is placed at the base of a group formed by some Salamandroidea members that are not closely related according to molecular studies and, as such, the position of *Wolterstorffiella* remains unclear. *Koalliella* forms a clade with *Lissotriton* (the only salamandrid scored in our matrix), grouped together by their pseudocoelous type of opisthocoely (see Auffenberg 1961; ch. 18) and the high neural crest (ch. 23). In our analysis based on the matrix from Macaluso et al. (2023), *Koalliella* is grouped with the Pleurodelinae (the "newts") and *Salamandrina* in a polytomy sharing ten apomorphies.

Caudata indet.
(Fig. 7)

Material: One dentary, MLU.GeoS.4028; Fig. 7a–d', one poorly preserved post-atlantal vertebra, MLU.GeoS.4021 (Fig. 7e–i'), one femur, MLU.GeoS.4020 (Fig. 7j–l').

Descriptions and remarks

Dentary: The bone is broken anteriorly and posteriorly, preserves a portion of the tooth-bearing region, and originated from a large-sized individual (Fig. 7a–d'). The outlines of both the broken anterior and posterior ends have semilunar shapes. In lingual view, up to 22 tooth positions corresponding to the tooth pedicles can be counted on the pars dentalis. The pedicels are anteroposteriorly compressed. In lingual view, the Meckelian groove is well pronounced. Anteriorly, it becomes shallower and almost closes, but deepens again along the anterior one-third of the preserved bone. The ventral flange of the bone is massive. The horizontal lamina is angular and the lingual surface of the bone is almost flat and vertical. Among the preserved salamander bones from Walbeck, this dentary belongs to the largest individual. Based solely on its large size, it could be referred to the largest salamander *Wolterstorffiella wiggeri* in the Walbeck assemblage.

Vertebra: A post-atlantal vertebra with a strongly eroded ventral surface is preserved, however, its centrum is clearly opisthocoelous (Fig. 7e–i'). The vertebra is strongly anterodorsally compressed. In dorsal view, the prezygapophyses are oval and extend parallel to the anteroposterior axis. The vertebral canal is rounded and has a horizontal ventral surface. The neural arch is almost flat. Due to its preservation, we could not define with confidence its anatomical position within the post-atlantal vertebral column. This could be a vertebra of *Koalliella*, however, the size of the above-described *Koalliella* vertebrae being anteroposteriorly half as long makes this assumption less probable. Due its poor preservation, a precise taxonomic identification is impossible and, for this reason, we conservatively assign it to Caudata indet.

Femur: The proximal portion of a femur (Fig. 7j–l') preserves the head and a broken diaphysis. The anteroposteriorly compressed and broad base of the trochanter is preserved. The proximal articulation portion of the bones is damaged. Only its posterior half is preserved. Its posterior surface is flat. Distally the bone slightly curves. As preserved, the femur most closely resembles femora of small-sized salamandrid genera (Sanchiz 1998a, b; Venczel 2000) and, based on its size, this femur could belong to the salamandrid *Koalliella genzeli*, but we identify it only as Caudata indet.

Although the three bones could be tentatively assigned to particular species of Walbeck salamanders, we prefer to conservatively describe them in open nomenclature as Caudata indet.

Anura Fischer, 1813
Palaeobatrachidae Cope, 1865
Palaeobatrachidae indet.
(Fig. 8)

Material: One maxilla, MLU.GeoS.4025 (Fig. 8a–f'), one sphenethmoid, MLU.GeoS.4024 (Fig. 8g–k) and 13 ilia, MLU.GeoS.4033 (Fig. 8o–q), MLU.GeoS.4034 (Fig. 8r–s'), MLU.GeoS.4035 (Fig. 8t, u), MLU.GeoS.4094,

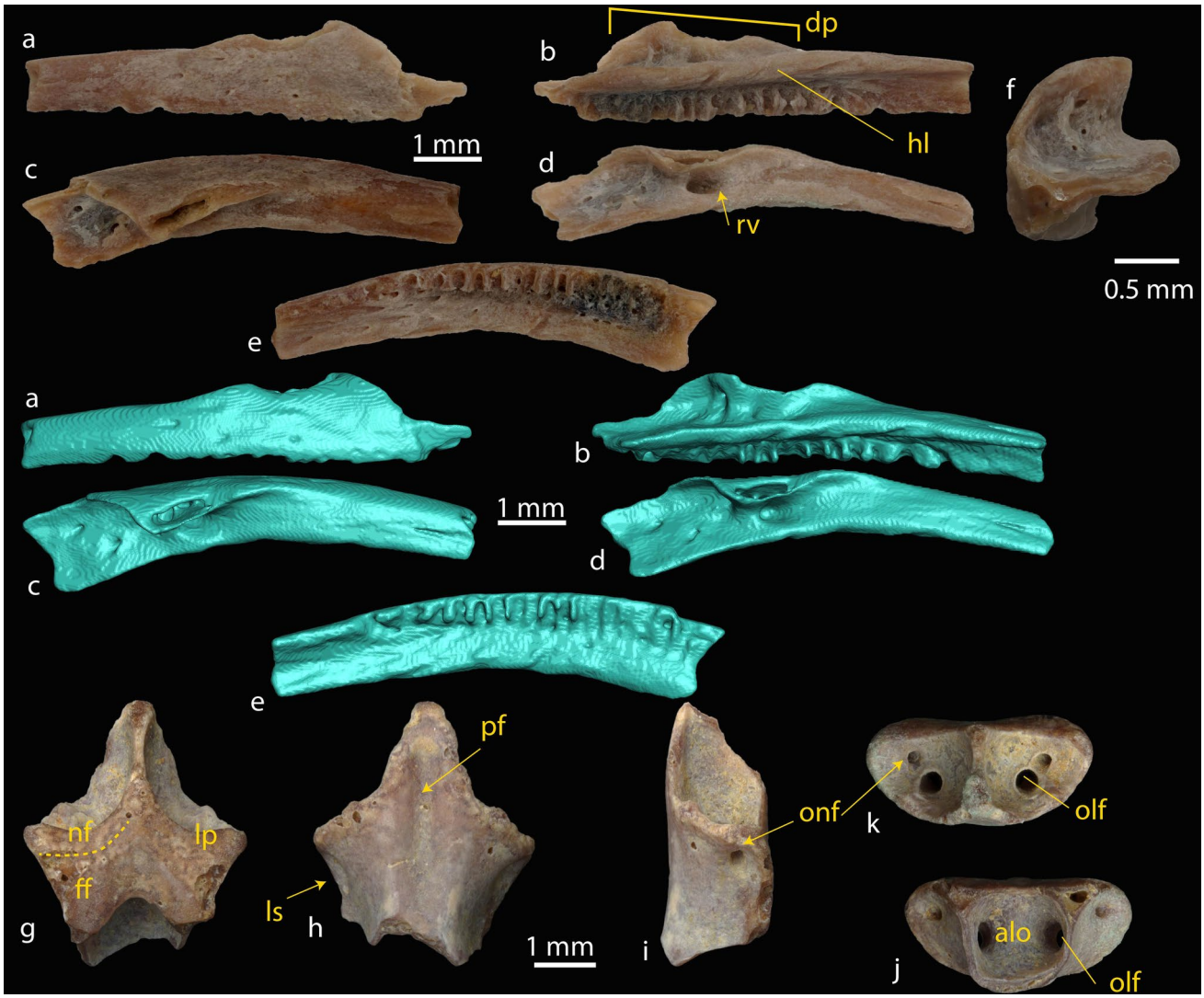

Fig. 8 Palaeobatrachidae indet. from Walbeck. **a–f'** MLU.GeoS.4025, maxilla, entire specimen in labial (**a**, **a'**), lingual (**b**, **b'**), dorsal (**c**, **c'**), dorsomedial (**d**, **d'**), ventral (**e**, **e'**), and anterior (**f**) views. **g–k** MLU.GeoS.4024, sphenethmoid, entire specimen in ventral (**g**), dorsal (**h**), left lateral (**i**), posterior (**j**), and anterior (**k**) views. **l–n** MLU.GeoS.4100, ilium, entire specimen in medial (**l**), posterior (**m**) and lateral (**n**) views. **o–q** MLU.GeoS.4033, ilium, entire specimen in lateral (**o**), posterior (**p**) and medial (**q**) views. **r–s'** MLU.GeoS.4034, ilium, entire specimen in lateral (**r**, **r'**) and medial (**s**, **s'**) views. **t**, **u** MLU.GeoS.4035, ilium, entire specimen in medial (**t**) and lateral (**u**). **v**, **w** MLU.GeoS.4096, ilium, entire specimen in lateral (**v**) and medial (**w**) views. The line separating nasal and frontoparietal facets is marked with dashed yellow line (**g**). Abbreviations: *alo* antrum pro lobo olfactorio; *dp* dorsal process; *ff* frontoparietal facet; *hl* horizontal lamina; *lp* lateral processes; *ls* lamina supraorbitalis; *nf* nasal facet; *onf* orbitonasal foramina; *olf* olfactory foramina; *pf* parasphenoid facet; *rv* recessus vaginiformis for processus maxillaris anterior of palatoquadrate bar. Specimens at different magnifications; see corresponding scale bars

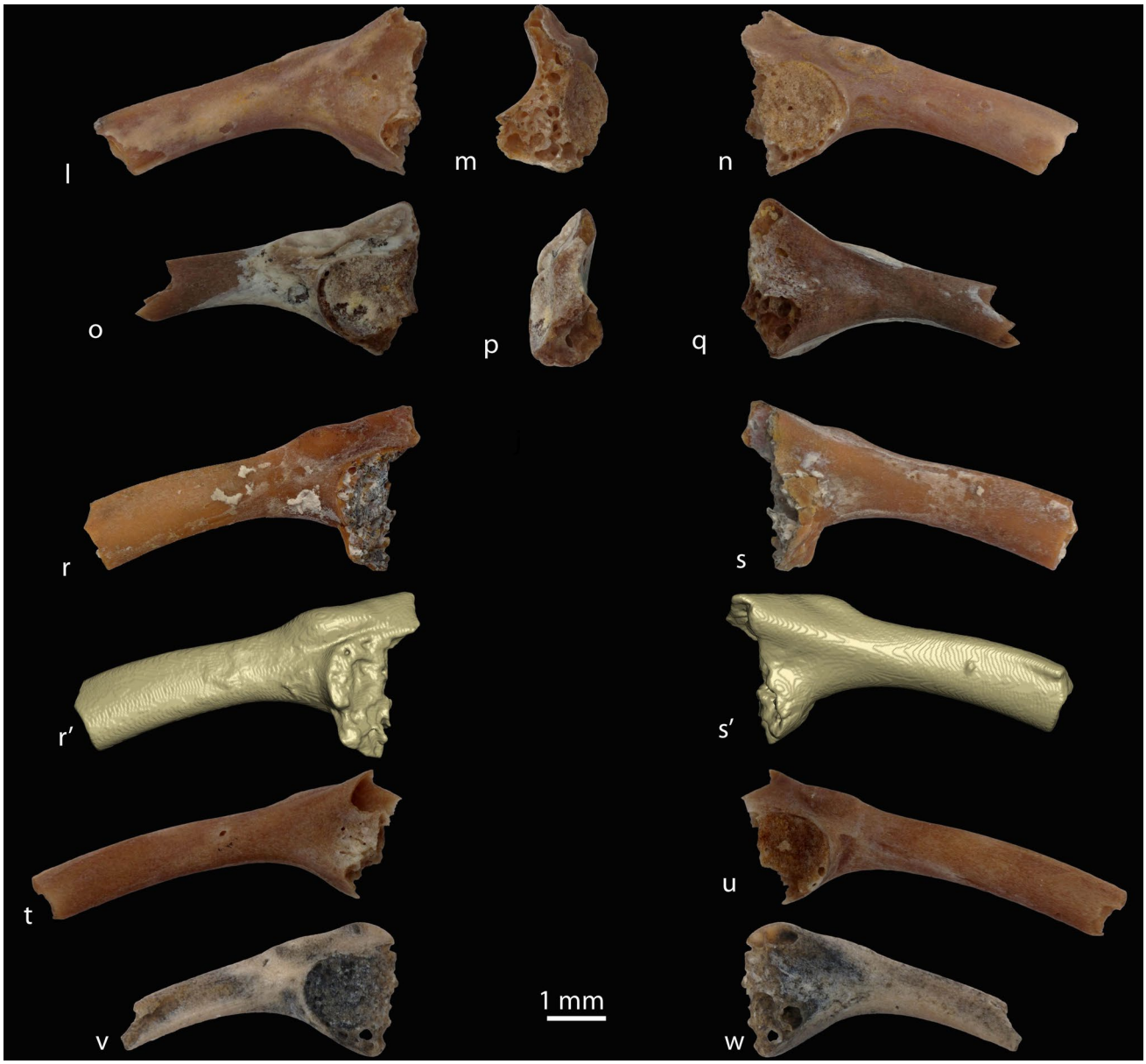

Fig. 8 (continued)

MLU.GeoS.4095, MLU.GeoS.4096 (Fig. 8v, w), MLU.GeoS.4097, MLU.GeoS.4098, MLU.GeoS.4099, MLU.GeoS.4100 (Fig. 8l–n), MLU.GeoS.4101, MLU.GeoS.4102, MLU.GeoS.4110.

Description and remarks

Maxilla: The available maxilla (Fig. 8a–f') is almost completely preserved. Laterally, the bone is dorsoventrally flattened and in ventral view it is anteroposteriorly curved. The dorsal process is broad anteroposteriorly and corresponds to less than half the length of the bone. The dorsal process is low, and, in anterior view, it has a curved (semilunar) outline (Fig. 8f). In dorsomedial view (Fig. 8d), a large foramen (corresponding to the recessus vaginiformis for processus maxillaris anterior of palatoquadrate bar) is visible at the corner between the highest tip of the dorsal process and the horizontal lamina. In lingual view, 17 tooth positions are observable on the pars dentalis (Fig. 8b). Only tooth bases are preserved and are anteroposteriorly compressed and oval in outline. The knob-like thickenings between tooth bases typical for palaeobatrachids are not present, which we interpret as a result of poor preservation. The horizontal lamina is well pronounced, projects lingually, and has a rounded labial surface (Fig. 8b, b'). The anterior tip of the bone is shallow and flat, almost lamina like.

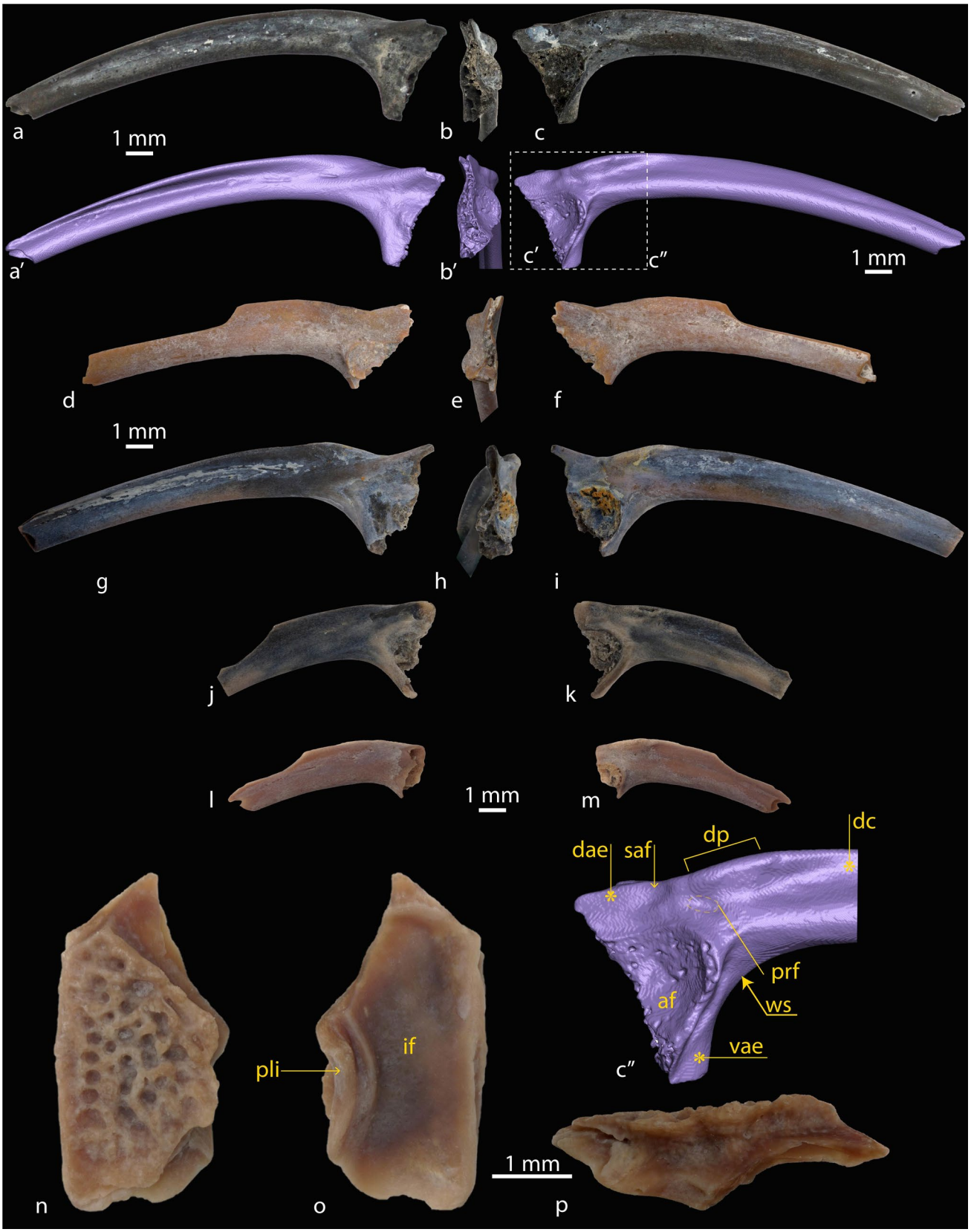
a
1 mm
b
c
a′
b′
c′
c″
1 mm
d
e
f
1 mm
g
h
i
j
k
l
1 mm
m
dae
saf
dp
dc
prf
ws
af
vae
c″
pli
if
1 mm
n
o
p

◂**Fig. 9** *Venczelibatrachus palaeocenicus* gen. et sp. nov. (**a**–**m**) and Pelobatidae indet. (?*Eopelobates* sp.) (**n**–**p**). *V. palaeocenicus*: **a**–**c''** MLU.GeoS.4029 (holotype), ilium, entire specimen in medial (**a**, **a'**), posterior (**b**, **b'**), and lateral (**c**, **c'**, **c''**) views, with **c''** showing close-up of the acetabular region and adjacent portion of shaft. **d**–**f** MLU.GeoS.4103 (paratype), ilium, entire specimen in lateral (**d**), posterior (**e**), and medial (**f**) views. **g**–**i** MLU.GeoS.4106 (paratype), ilium, entire specimen in medial (**g**), posterior (**h**), and lateral (**i**) views. **j**, **k** MLU.GeoS.4108 (paratype), ilium, entire specimen in medial (**j**) and lateral (**k**) views. **l**, **m** MLU.GeoS.4109 (paratype), ilium, entire specimen in medial (**l**) and lateral (**m**) views. Pelobatidae indet. (?*Eopelobates* sp.): **n**–**p** MLU.GeoS.4022, frontal/frontoparietal, entire specimen in dorsal (**n**), ventral (**o**), and lateral (**p**) views. The preacetabular fossa is highlighted with dashed yellow line (**c''**). Abbreviations: *af* acetabular facet; *dae* dorsal acetabular expansion; *dc* dorsal crest; *dp* dorsal prominence; *if* incrassatio frontoparietalis; *pli* processus laterialis interior; *prf* preacetabular fossa; *saf* supraacetabular fossa; *ws* wing–like structure; *vae* ventral acetabular expansion. Specimens at different magnifications; see corresponding scale bars, only c'' is not scaled

Sphenethmoid: The preserved sphenethmoid is compact and relatively gracile (Fig. 8g, h). The parasphenoid facet is shallow and deepens slightly anteriorly. The lateral processes are present, but both are broken. The lateral processes project anterolaterally, but they are not especially prominent (Fig. 8g, h). The nasal facets are broad and shallow. The lengths of the frontoparietal and nasal facets are equal. In anterior view, large olfactory and small orbitonasal foramina are visible (Fig. 8j). The latter is located above the former. In posterior view, the olfactory foramina are visible too, located within the antrum pro labo olfactorio (Fig. 8k). The orbitonasal foramen is visible on the lateral wall of the bone, in the corner at the fusion of the lateral process and lamina supraorbitalis (Fig. 8i).

Ilium: The ilia (Fig. 8l–w) preserve a portion of the iliac body and the adjacent portion of the shaft. The ilia are robust. The iliac body is moderately large. The acetabular fossa occupies most of the lateral surface of the iliac body (Fig. 8n, x). It is twice as high as the iliac shaft. The iliac shaft is round in cross-section and arch shaped. Laterally, a shallow preacetabular fossa is visible at the base of the iliac shaft. The anterior margin of the acetabular facet is high, whereas the dorsal and anteroventral margins are low. The dorsal acetabular expansion is well developed, whereas the ventral one is absent. The lateral surface of the dorsal acetabular expansion is mainly flat. It possesses a fossa located either at the anterior base of the dorsal acetabular expansion or between the anterior base of the dorsal acetabular expansion and dorsal prominence. The dorsal margin of the dorsal acetabular expansion either mostly creates an obtuse angle (e.g. Fig. 8o, q) or rarely is in a line with the dorsal margin of the iliac shaft (Fig. 8r, s). The dorsal prominence is elongate and not high. Its surface can be uneven, but does not form any significant structures resembling the dorsal protuberance. The medial surface of the bone is indented by a deep, triangular depression (Fig. 8l, y), which provides a curved outline to the ilioischiadic juncture in posterior view (e.g. Fig. 8p).

Remarks: The described remains can be attributed to the family Palaeobatrachidae based on: in ventral view, the sphenethmoid possesses the articulation area delimited by two parallel ridges for contact with the parasphenoid, and a short septum nasi and lateral process; and the ilium bears an acetabular facet that is large with a convex articulation surface; and the medial surface of the iliac body possess a prominent convexity (Vergnaud-Grazzini and Młynarski 1969; Vergnaud-Grazzini and Hoffstetter 1972; Wuttke et al. 2012). The maxilla resembles the morphology described and illustrated by Villa et al. (2016: fig. 2M) for *Palaeobatrachus eurydices*, especially in the dimension and location of the recessus vaginiformis for receipt of the processus maxillaris anterior of the palatoquadrate bar. Among the palaeobatrachid genera, the Walbeck form can be distinguished from *Albionbatrachus* by the lack of the small tubercle on the preacetabular portion of the ilium. Because the species-level taxonomy of Palaeobatrachidae is based on the morphology of the frontoparietal bone (Roček et al. 2015), which is missing in the Walbeck collection, the Walbeck palaeobatrachids can only be identified to the family level.

Alytidae Fitzinger, 1843
Venczelibatrachus nov. gen.
urn:lsid:zoobank.org:act:9E0AED62-FDAE-4C8A-884C-18FF08A8C6C8

Type species: *Venczelibatrachus palaeocenicus*, only species in the genus.
Etymology: The generic name combines the surname of a Romanian herpetologist Dr. Márton Venczel, with the Greek-derived suffix "batrachus", meaning an anuran.
Diagnosis: As for species.

Venczelibatrachus palaeocenicus nov. sp.
urn:lsid:zoobank.org:act:1272F27B-0C60-4879-AFA4-AA85B51233C5
(Fig. 9a–m)

Holotype: A nearly complete left ilium, MLU.GeoS.4029 (Fig. 9a–c'').
Paratypes: Seven ilia: MLU.GeoS.4103 (Fig. 9d–f), MLU.GeoS.4104, MLU.GeoS.4105, MLU.GeoS.4106 (Fig. 9g–i), MLU.GeoS.4107, MLU.GeoS.4108 (Fig. 9j, k), MLU.GeoS.4109 (Fig. 9l, m).
Etymology: The species is named for the Palaeocene epoch, the time when this new frog genus and species lived.
Type locality, horizon and age: Walbeck fissure filling within Muschelkalk limestone (precise position unknown), Sachsen-Anhalt State, Germany; MP 1–5, probable middle Selandian, Palaeocene (Weigelt 1939; De Bast et al. 2013; De Bast and Smith 2016).
Diagnosis: Differs from all other alytids in the following unique combination of iliac features: well-developed dorsal

crest; elongate and low dorsal prominence with smooth surface; both dorsal crest and dorsal prominence laterally bent; poorly-developed supraacetabular fossa; iliac shaft and iliac body are connected by a wing-like thin lamina; and ventral acetabular expansion relatively well developed.

Description (based on the holotype if not otherwise specified) and remarks

Ilium: The ilium (Fig. 9a–m) has a relatively small iliac body and long iliac shaft. The acetabular facet is moderately developed and has an irregular hemispheric outline (Fig. 9c, d, i). The anterior margin of the facet is prominently expanded laterally, whereas the other parts are not as prominent. The dorsal acetabular expansion is high along its posterior portion and has a broad base. The ventral acetabular expansion is present, but weakly developed. In the best-preserved specimens, the dorsal expansion is around four times as large as the ventral expansion. The supraacetabular fossa is small and located at the anterior base of the dorsal acetabular expansion. The iliac shaft possesses a well-developed dorsal crest that extends along almost the entire length of the shaft (Fig. 9c, i). The surface for the attachment of the m. iliacus externus (sensu Přikryl et al. 2009) is weakly developed. Posteriorly, the dorsal crest possesses a rather elongate, but poorly developed (i.e. low) dorsal prominence with an almost smooth surface. Both the dorsal crest and dorsal prominence are laterally inclined. The ventral base of the iliac shaft (= posteroventral portion of the iliac shaft) possesses a low lamina resembling a wing-like structure that connects with the preacetabular zone of the iliac body (Fig. 9a). The large but shallow preacetabular fossa is located in the corner between the iliac shaft and iliac body. The medial surface of the iliac body is indented by an almost triangular and relatively shallow depression (e.g. Fig. 9f, g). In well-preserved specimens, the ilioischiadic juncture is narrow and extends slightly ventrally (Fig. 9b, e).

Remarks and comparison: The ilia can be assigned to Alytidae based on general morphology and bone dimensions, by the presence of the dorsal protuberance, well-developed dorsal acetabular expansion, and weakly developed to almost absent ventral acetabular expansion (Roček 1994; Venczel et al. 2016). Following Venczel et al. (2016), we consider Alytidae to contain following fossil and recent genera: *Alytes, Bakonybatrachus, Discoglossus*, *Enneabatrachus, Eodiscoglossus, Iberobatrachus, Kizylkuma, Latoglossus, Latonia, Paradiscoglossus, Paralatonia, Wealdenbatrachus. Venczelibatrachus palaeocenicus* can be distinguished from *Alytes, Enneabatrachus, Iberobatrachus* and *Kizylkuma* by the presence of a well-developed dorsal crest and from *Bakonybatrachus*, *Discoglossus, Eodiscoglossus*, *Latonia, Paradiscoglossus*, *Paralatonia*, and *Wealdenbatrachus* by a poorly developed supraacetabular fossa. The dorsal prominence in *V. palaeocenicus* is weakly developed in comparison to *Alytes*, *Discoglossus*, *Eodiscoglossus*, *Kizylkuma*, *Latonia*, *Latoglossus*, *Paradiscoglossus*, and *Paralatonia*, but closely resembles *Wealdenbatrachus* from Spain in its shape and degree of development. *Venczelibatrachus palaeocenicus* shows the following exclusive characters, which are not observed in any known alytid: the presence of a low lamina resembling a wing–like structure at the ventral base of the iliac shaft (= posteroventral portion of the iliac shaft) and connecting with preacetabular zone; the dorsal crest and dorsal prominence are bent laterally and the transition from one to another is almost invisible; the dorsal prominence has an almost smooth surface; and in comparison to all other fossil and recent alytids has a better-developed ventral acetabular expansion. Although variation is evident in the figured ilia of *V. palaeocenicus*, all of them share the above-listed characteristic features.

Venczelibatrachus palaeocenicus has a unique combination of characters among all known alytids, both from North America and Europe. Its ilium morphology is most similar to *Paradiscoglossus americanus* from the latest Cretaceous of North America (Estes and Sanchíz 1982b; Gardner 2008; Gardner and DeMar 2013) in the shape and dimensions of the bone, as well as the presence of a thin, wing-like lamina between the iliac shaft and ventral acetabular expansion, and an elongate and low dorsal prominence. However, it differs from the North American species by the presence of a small supraacetabular fossa, better pronounced ventral acetabular expansion, smooth dorsal prominence, and dorsolaterally bent dorsal crest. Further similarities with another Late Cretaceous alytid from Hungary, *Bakonybatrachus fedori* (Szentesi and Venczel 2012), are a thin, wing-like lamina (which is, however, smaller than in *V. palaeocenicus*) between the iliac shaft and ventral acetabular expansion, a small supraacetabular fossa, and a low and elongate dorsal prominence. However, in *B. fedori* the ventral acetabular expansion is absent and the dorsal crest is dorsomedially bent. The unique ilium morphology of *V. palaeocenicus* suggests a hidden early Palaeogene diversity for alytids.

Pelobatidae Bonaparte, 1850

Pelobatidae indet. (?*Eopelobates* sp.)
(Fig. 9n–p)

Material: One frontal/frontoparietal, MLU.GeoS.4022 (Fig. 9n–p).

Description and remarks

Frontal/Frontoparietal: The sole example (Fig. 9n–p) is a rectangular, flattened bone. Whether the bone represents a

frontal or a frontoparietal cannot be stated due to its fragmentary preservation. The dorsal surface possesses dermal ornamentation consisting of a pit-and-ridge pattern. The pits are round, partially merge into each other, and also form grooves. The same ornamentation can be found in the pelobatid *Eopelobates* (Roček et al. 2014). The ornamented surface is elevated, but posteriorly, laterally and anteriorly, the unornamented bone margins form flanks that project ventrally. The ventral surface of the bone is smooth and slightly concave, which we interpret as the incrassatio frontoparietalis. Laterally, the ventral surface is flanked by a shallow ridge having a semilunar shape. It forms the medial wall of a shallow duct, the lateral wall of which is well pronounced and projects ventrally. We interpret that structure as the processus lateralis interior of the pars contacta. The lateral margin of the bone possesses a ventrally projecting crest. Similar morphology and bone dimensions can be found in pelobatid frogs (e.g. Roček et al. 2014: fig. 8a). The smooth, medial margin of the bone appears to be intact, suggesting that the paired frontals/frontoparietals were not fused, but whether it comes from an adult individual cannot be stated. The observed dermal ossification is found in both juvenile and adult individuals of the family Pelobatidae (Roček et al. 2014). Other frog groups with dermal ossification on their frontal/frontoparietal such as the genus *Latonia* (Vasilyan 2020) and family Palaeobatrachidae (Roček et al. 2015, 2021) can be excluded, because both juvenile and adult forms do not have any similar ornament. Further, in *Latonia* the ornamentation of the skull roof is a secondary exostosis fused to the surface of the dermal bone (e.g. Roček 1994). Similar ornamentation can also be found in *Thaumastosaurus,* but the morphology of the frontal in this genus is significantly dissimilar to the Walbeck specimen (Vasilyan 2018: fig. 2T–Y). Furthermore, *Thaumastosaurus* has been suggested to be a mid-Eocene immigrant from Africa (Vasilyan 2018). Thus, most probably, the bone can be attributed to the family Pelobatidae and probably to the genus *Eopelobates*. However, further and more diagnostic fossils will be necessary to confidently confirm the presence of the family and genus in Walbeck.

Anura indet.
(Fig. 10a–u)

Material: Ten vertebrae, MLU.Geo.4083 (Fig. 10a–d), MLU.Geo.4084 (Fig. 10e–i), MLU.Geo.4085, MLU.Geo.4086, MLU.Geo.4087 (Fig. 10o–s), MLU.Geo.4088, MLU.Geo.4089, MLU.Geo.4090, MLU.Geo.4091, MLU.Geo.4092 (Fig. 10j–n), and one radioulna, MLU.GeoS.4111 (Fig. 10t, u).

Descriptions and remarks

Vertebrae: Ten anuran postatlantal vertebrae are available from Walbeck. Among them, three morphotypes can be identified.

Morphotype 1 (Fig. 10a–i): Four opisthocoelous vertebrae (MLU.Geo.4083–4086) with a dorsoventrally flattened centrum are the largest available vertebrae. The anterior condyle is short. The neural arch is thin and its dorsoanterior margin is flat. No foramina can be observed in the arch. The pre- and postzygapophysis are small and rounded to slightly elongate. MLU.Geo.4083 (Fig. 10a–d), the largest vertebra, bears a large and massive transverse process that is oriented laterally and slightly posteriorly. The distal tips of the processes are uneven, suggesting that they served as an articulation/attachment surface with ribs (costae) (Roček 1994). This morphotype resembles trunk vertebrae of the alytid *Latonia* (Roček 1994) in general morphology and in having an opisthocoelous centrum and large transverse processes probably articulating with ribs.

Morphotype 2 (Fig. 10j–n): Five procoelous, small-sized vertebrae (MLU.Geo.4088–4092) bearing gracile transverse processes and a thin neural arch. In dorsal and ventral views, the vertebrae have rectangular outlines, being laterally broader than anteroposteriorly elongate. The vertebral canal has a round outline. The pre- and postzygapophyses are tiny and round. Procoelous vertebrae are known in both Palaeobatrachidae (Wuttke et al. 2012) and Pelobatidae (Roček et al. 2014).

Morphotype 3 (Fig. 10o–s): One vertebra (MLU.Geo.4087) with bicondylar (posterior) sacro-urostylar and unicondylar (anterior) articulations. The vertebral canal is dorsoventrally compressed. The postzygapophyseal region is massive and projects posterodorsally. The preserved bases of the transverse processes suggest those were not massive. A comparable morphology can be observed within alytid frogs (Roček 1994; Biton et al. 2016; Venczel et al. 2016). Based on their alytid-like forms, morphotypes 1 and 3 may belong to *Venczelibatrachus palaeocenicus*. However, a complete skeleton will be necessary to verify that assignment.

Radioulna: The preserved radioulna (MLU.GeoS.4111) is large and long (Fig. 10t, u). The grooves on both the dorsal and ventral surfaces are not deep. The calcified articular cartilage is almost inexistent. The width of the diaphysis is half the length of the distal end of the bone. The capitulum and olecranon are not prominent, but collectively form an obtuse angle. No foramina or fossa are observable at the base of the proximal articulation portion (capitulum and olecranon).

Figured radioulna in the literature are extremely rare, making comparison and further identification challenging. Our comparisons with known members of the families (Alytidae, Palaeobatrachidae, Pelobatidae) present in the Walbeck assemblage suggests the shallow groove on the dorsal surface of the bone, lack of fossa and foramina at the base of the proximal articulation portion, and general bone dimensions of the Walbeck radioulna are most similar to Alytidae, especially *Alytes* and *Latonia* (Bastir et al. 2014;

Fig. 10 Lissamphibian and reptilian remains from Walbeck. **a**–**u** Anura indet.: **a**–**d** MLU.Geo.4083, Morphotype 1, trunk vertebra, entire specimen in anterior (**a**), posterior (**b**), dorsal (**c**), and ventral (**d**) views; **e**–**i** MLU.Geo.4084, Morphotype 1, trunk vertebra, entire specimen in anterior (**e**), posterior (**f**), dorsal (**g**), ventral (**h**), and left lateral (**i**) views; **j**–**n** MLU.Geo.4092, Morphotype 2, trunk vertebra, entire specimen in anterior (**j**), posterior (**k**), dorsal (**l**), ventral (**m**), and right lateral (**n**) views; **o**–**s** MLU.Geo.4087, Morphotype 3, sacral vertebra, entire specimen in anterior (**o**), posterior (**p**), dorsal (**q**), ventral (**r**), and right lateral (**s**) views; **t**, **u** MLU.GeoS.4111, radioulna, entire specimen in posteroventral/medial (**t**) and anterior (**u**) views. **v**–**x** Lissamphibia indet.: MLU.GeoS.4026, maxilla fragment, entire specimen in labial (**v**), and lingual (**x**) views. **y**, **z** Crocodylia indet.: **y**, MLU.GeoS.4121, osteoderm in dorsal view; **z** MLU.GeoS.4123, osteoderm in dorsal view. **za**, **zb** Testudines indet.: MLU.GeoS.4024, costal in dorsal (**za**) and ventral (**zb**) views. Specimens at different magnifications; see corresponding scale bars

Biton et al. 2016; Vasilyan 2020). MLU.GeoS.4111 differs from palaeobatrachids, which have extensive grooves in the radioulna and larger olecranon (Venczel 2004; Bastir et al. 2014; Villa et al. 2016) and from pelobatids, which have massive and short radioulna (Bailon 1999). Although MLU.GeoS.4111 may belong to the alytid *Venczelibatrachus palaeocenicus*, we prefer to conservatively identify the fossil as belonging to Anura indet.

Lissamphibia indet.
(Fig. 10v–x)

Material: one maxilla fragment, MLU.GeoS.4026 (Fig. 10v–x).

Description and remarks

The preserved maxilla fragment is gracile. The horizontal lamina is rather well developed. The pars dentalis possesses more than ten tooth pedicel traces. The labial surface of the bone is smooth. Due to its poor preservation, taxonomic assignment of the fragment to either frogs or salamanders cannot be confidently made.

Crocodylia Gmelin, 1789

Crocodylia indet.
(Fig. 10y, z)

Material: three osteoderms, MLU.GeoS.4121 (Fig. 10y), MLU.GeoS.4122, MLU.GeoS.4123 (Fig. 10z).

Description and remarks

Osteoderms are up to 3 cm large. Their internal surfaces are smooth, whereas the external is covered with a sculpture made of circular or semicircular deep and well-pronounced pits. None of the osteoderms can be identified beyond Crocodylia indet.

Testudines Batsch, 1788

Testudines indet.
(Fig. 10za, zb)

Material: one costal MLU.GeoS.4024 (Fig. 10za, zb).

Description and remarks

The only available turtle bone is a fragmentary costal. The lateral margins are broken. The dorsal surface is uneven and covered with a network of shallow pits and ridges. Unfortunately, the bone does not display any diagnostic characters, which hinders further taxonomic identification.

Discussion

The Walbeck lissamphibian fauna includes three salamanders (*Wolterstorffiella wiggeri*, *Geyeriella mertensi*, and *Koalliella genzeli*) and three frogs (Palaeobatrachidae indet., the new alytid genus and species *Venczelibatrachus palaeocenicus*, and a pelobatid tentatively identified as ?*Eopelobates*). The reptilian fauna includes three lizards (Lacertidae indet., *Camptognathosaurus walbeckensis*,?Scincoidea indet., all recently published by Čerňanský and Vasilyan (2024)), a crocodile (Crocodylia indet.) and a turtle (Testudines indet.). In total, the Walbeck herpetofauna includes at least eleven taxa. As such, the Walbeck site, together with Cernay (Estes et al. 1967; Rage 2003), provides valuable insights into the Palaeocene taxonomic diversity of amphibians and reptiles in Europe.

The fossil assemblage of salamanders at Walbeck is especially exceptional, given the rarity of Palaeocene localities yielding salamanders remains in Europe. It contains the large-sized *Wolterstorffiella wiggeri* and the smaller-sized *Geyeriella mertensi* and *Koalliella genzeli* (Fig. 3).

Wolterstorffiella wiggeri is unique to the Walbeck site. Estes (1981) regarded the species as a Dicamptodontinae, based on similarities "in vertebral proportions" (Estes 1981: p. 49). A recent study suggested that *W. wiggeri* might be a putative cryptobranchoid, pending whether first-hand observations of the material could confirm intervertebral spinal nerve exit along the column (Macaluso et al. 2022b). The morphological characters of *Wolterstorffiella*, especially the presence of spinal nerve foramina in some of the vertebrae, which exclude the previously suggested cryptobranchoid attribution, indicate *W. wiggeri* belongs to superfamily Salamandroidea. Our vertebrae-based phylogenetic analyses were not able to resolve the family-level taxonomy of *W. wiggeri*. It is placed as a basal taxon of the clade containing extant *Dicamptodon* and *Ambystoma* and fossil sirenids and batrachosauroids (*Habrosaurus* and *Opisthotriton* and *Prodesmodon* respectively in Fig. 6). Articulated and/or other bones of *Wolterstorffiella* are necessary to better assess its phylogenetic position.

The proteid *Geyeriella mertensi* is the oldest record of the family in the European continent. Although the family is known from the Late Cretaceous of both North America and Asia, prior to our study their earliest European record was in the early Oligocene (Macaluso et al. 2022a; Skutschas et al. 2024). Interestingly, another species of *Geyeriella*, *G. wettsteini*, is known from the Devinská Nová Ves site (Slovakia, Middle Miocene) (Herre 1955), suggesting the genus is a Lazarus taxon with a hidden fossil record of around 45 Ma years. Another example of a Lazarus taxon among European salamanders is *Palaeoproteus*, whose species have a similar, extremely patchy fossil record in Europe spanning

from the Palaeocene to the Late Pliocene (Estes et al. 1967; Vasilyan and Yanenko 2020; Villa et al. 2024). *Geyeriella* together with other European proteids (*Euronecturus, Mioproteus*, *Proteus*) suggests that the family was diverse during the Cenozoic and represented by several putative lineages. However, their precise phylogenetic position within the family requires further analysis of more complete remains. The intriguing fact that *Geyeriella*, as a stem proteid dates to the Palaeocene of Europe, whereas the oldest crown proteid *Bishara* is from the Late Cretaceous of Asia (Skutschas et al. 2024) suggests the family was more diverse and widespread in the past. Apparently, in the late Mesozoic, the family diversified and was represented in different continents (North America, Europe, and Asia) by different clades. *Geyeriella* is a candidate for the first diversification episode of stem proteids, which Skutschas et al. (2024) suggested occurred in the Late Jurassic and was followed by dispersal into North America and Asia. These interpretations should be considered tentative taking into account the facts that: 1) the phylogenetic analysis (present paper), on which the interpretations are made, is based only on vertebral characters and 2) proteid pre-Quaternary fossil records in North America and Asia are less understood. In North America, the published proteid fossil record is especially poor compared to the European one, with the former represented by rare vertebrae from the latest Cretaceous and Palaeocene (Naylor 1978; DeMar 2013; Wilson et al. 2014).

The small-sized *Koalliella genzeli* differs from other Walbeck salamanders in having a relatively continuous presence in European Palaeocene sites (Table 2) and either this species or a closely related one may also be present from the early (Silveirinha, Portugal: Rage and Augé 2003) to late Eocene (personal observations of DV). Our phylogenetic analyses support the assignment of *Koalliella* to Salamandridae and nested within "Pleurodelinae" (Fig. 6d). *Koalliella* represents the oldest member of Salamandridae, suggesting a long palaeobiogeographic history for the family on the European continent.

Although the Palaeocene salamander record in Europe is limited (Table 2), some palaeobiogeographic observations can be made. At least three salamander families (Batrachosauroididae, Proteidae, Salamandridae) and a further large-sized Salamandroidea (*Wolterstoffiella*) are present in the Palaeocene of Europe. These families have Laurasian origins and thus, their Mesozoic "roots" can be assumed. All these Walbeck salamander species are limited to the Cenozoic and can thus be regarded as Cenozoic taxa. Surprisingly, the genus *Palaeoproteus* is not present in the Walbeck fauna, although it is the most "common" taxa in other European Palaeocene sites (Table 2). Its absence at Walbeck may be the result of local provincialism (the most northeastern Palaeocene site) or sampling bias. A further salamander, Ambystomatoid indet., has been reported from the late Palaeocene age site of Rivecours, France (Smith et al. 2014). Further study/identification of that intriguing report is necessary to establish its identity and palaeobiogeographic significance.

Comparisons with the Palaeocene North American and Asian records highlight the unique position of the European salamander record. In Asia during the Palaeocene, only cryptobranchid (Gubin 1991) and hynobiid (Van Itterbeeck et al. 2007) families have been recorded. The North American record is more diverse and includes cryptobranchids, proteids, batrachosauroidids, scapherpetontids, amphiumids, and sirenids (Gardner 2003a, b, 2012; Gardner and DeMar 2013). The North American Palaeocene salamander fauna is quite segregated from the European fauna, with the presence of different genera and species of batrachosauroidids and three families (amphiumids, scapherpetontids, and sirenids) completely absent from European assemblages. As mentioned above, the proteids are much less diverse and abundant in the Palaeogene of North America compared to the Palearctic region (Vasilyan et al. 2017; Macaluso et al. 2022a). Salamandridae has a rather abundant fossil record in the Palaeogene of Europe, but only appears later in the North American fossil record in the Oligocene onwards (Jacisin and Hopkins 2018). Lacking any batrachosauroidid taxon, contrary to other Palaeocene European faunas, such as Cernay and Hainin (Estes et al. 1967; Groessens-Van Dyck 1981a, b), the Walbeck assemblage is even more unique and different from the ones occurring during the Palaeocene in North America (e.g. Estes 1976), showing a clear segregation at least in the salamander components of the fauna.

Walbeck frogs are represented by three families: Palaeobatrachidae, Alytidae, and Pelobatidae (Table 2). The first two families are commonly found in European Palaeocene (Table 2) and Cretaceous assemblages, and they represent typical European Mesozoic clades (e.g. Blain et al. 2010; Venczel et al. 2016).

Palaeobatrachidae were present in Europe, since the Late Cretaceous (sites in Spain and France; Buffetaut et al. 1996; Blain et al. 2010), however, the generic attribution of those records remains unclear. Prior to our report, the Palaeocene record of the family was limited to *Palaeobatrachus* from Cernay, France, and an unidentified record from Hainin, Belgium (Table 2). The family becomes abundant in Europe starting in the Eocene (Roček et al. 2021). The Laurasian Palaeobatrachidae are considered to have evolved from the Gondwanan pipoids (Wuttke et al. 2012). If their European Cretaceous record is undoubted (Buffetaut et al. 1996), the North American record needs to be confirmed by unquestionable palaeobatrachid elements. The few palaeobatrachid records from North America (Estes and Sanchíz 1982b: fig. 1C–F; Gardner 2008: fig 13.1 A–B) have been suggested to belong to other frog groups (e.g. Wuttke et al. 2012; Roček et al. 2021). The Walbeck find extends their

Table 2 Lissamphibian fauna of Palaeocene sites in Europe. Occurrences at Walbeck are bolded

	Locality	Hainin	**Walbeck**	Cernay-lès-Reims, Lemoine Quarry	Cernay-lès-Reims, Mt. Berru, Mouras Quarry	Rivecourt, Petit Pâtis Quarry
	MP	MP1–5	**MP1–5**	MP6	MP6	MP6b
	Age	Early–middle Palaeocene	**Early–middle Palaeocene**	Late Palaeocene	Late Palaeocene	Latest Palaeocene
	References	Groessens-Van Dyck 1981a, 1981b; Rage and Roček 2003	**this study**	Estes et al. 1967; Rage 2003; Rage and Roček 2003; Roček and Rage 2000; Vergnaud-Grazzini and Hoffstetter 1972	Estes et al. 1967	Smith et al. 2014
Caudata	*Palaeoproteus gallicus*	+		+	+	
	cf. *Salamandra* sp.			+		
	cf. Salamandridae indet.	+				
	Koalliella genzeli	cf.	+			
	Koalliella sp.			+		
	Wolterstorffiella wiggeri		+			
	Geyeriella mertensi		+			
	Ambystomatoid indet.					+
Anura	Bufonidae indet.			+		
	Palaeobatrachus sp.			+		
	Palaeobatrachidae indet.	+	+			
	Venczelibatrachus palaeocenicus		+			
	Alytidae indet.	+				
	Pelobatidae indet. (?*Eopelobates*)		+			
	Anura indet.			+		

Palaeocene distribution slightly to the east. Only later, since the Eocene, did palaeobatrachids disperse eastwards, reaching Eastern Europe (Wuttke et al. 2012).

The distinct alytid, which we have described herein as the new genus and species *Venczelibatrachus palaeocenicus*, is the first European Palaeocene alytid species. The family had been reported from the Hainin site (Table 2), however, without a clear generic attribution. Alytids were the most diverse European frog family during the Cretaceous, where they are known by several genera and species (Venczel et al. 2016). Their later Palaeocene–Eocene record is poorly understood, with extremely scarce fossil records being at best identified at the family level (e.g. Hainin: Table 2; Dormaal: Godinot et al. 1978; Prémontré:

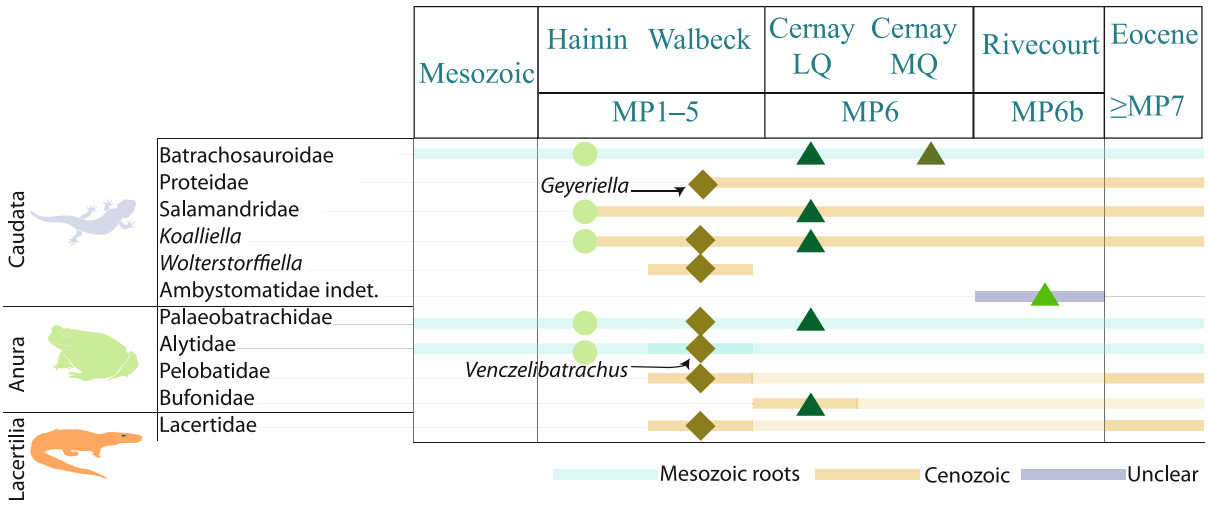

Fig. 11 Stratigraphic distribution of Walbeck and other Palaeocene taxa (Table 1) from the late Mesozoic to the early Eocene of Europe. Their stratigraphic distribution is marked by different colours depending on their occurrences (Mesozoic, exclusively Cenozoic, or unknown). Abbreviations: *LQ* Lemoine Quarry; *MQ* Mouras Quarry

Augé et al. 1997). Considering the rich Cretaceous and post Eocene record of the family in Europe, there is good reason to suspect that the family was represented in Palaeocene–Eocene by forms that await discovery.

Prior to our study, Pelobatidae had not been documented in the Palaeocene (Table 2, Fig. 11). Although the generic attribution of the Walbeck specimen is not certain, it can be assigned to the family. The earliest pelobatids (*Eopelobates*) are known from the Cretaceous of North America (Roček et al. 2014). Previously, the oldest European record for the family was in the early Eocene (MP 7, Silveirinha, Portugal: Rage and Augé 2003; Rage 2012), whereas the oldest *Eopelobates* is younger and dates to MP 10 (Prémontré, France: Roček et al. 2014). The Walbeck find indicates that the family was already present in Europe earlier in the Palaeocene and probably dispersed from North America earlier than the Eocene, as previously thought. If the identification of the Walbeck frontal/frontoparietal (MLU.GeoS.4022, Fig. 9n–p) as *Eopelobates* is confirmed by future finds, it will extend the temporal range of the genus. The only other report of a frog family in the Palaeocene of Europe is two ilia and one pterygoid from Cernay, France, that Rage (2003) assigned to Bufonidae. That occurrence was considered palaeobiogeographically unexplained because the Laurasian fossil record of the family is limited to the Neogene of North America, Asia, and Europe (Roček 2013), and Cretaceous and other Palaeogene records are unknown. It is plausible that bufonids were present in the early Cenozoic, but have yet to be discovered.

The herein described two new reptilian taxa (Crocodylia indet., Testudines indet.) are unfortunately not informative to compare with other known records. However, together with three lizards (Čerňanský and Vasilyan 2024), they expand the reptilian fauna of Walbeck.

Conclusions

As previously proposed, the major faunistic shift of lissamphibians in Laurasia happened during the Palaeocene, once most of the K-Pg survivors (European Discoglossidae and Palaeobatrachidae may be an exception) and new lineages (such as the Bufonidae, Rhinophrynidae, Salamandridae) were established (Rage 2012; Roček 2013). Our study of the Walbeck herpetofauna, considered lost to science for several decades, complements the poorly known Palaeocene liss-amphibian fauna of Europe and provides insight into the palaeobiogeographic history of frogs and salamanders during the Palaeocene (Fig. 11). The salamander assemblage includes the large-sized *Wolterstorffiella*, probably related to the extant clade of Dicamptodontidae and Ambystomatidae, two families confined to present-day North America, suggesting a strong palaeobiogeographic link between the North American and European continents. The two other Walbeck salamanders, *Geyeriella* and *Koalliella*, are smaller in size and are the oldest records in Europe of Proteidae and Salamandridae, respectively, suggesting a long history for these families in Europe. The frog fauna includes two forms known from the Cretaceous, Palaeobatrachidae and Alytidae, and the latter is represented by a new genus and species, suggesting their probable survival from the Mesozoic. The third taxon is a spadefoot toad (Pelobatidae indet. (?*Eopelobates* sp.)) and represents the oldest record for the family in Europe, which previously had been dated as MP 7 (Rage 2012).

To summarise, as also demonstrated by the lizard fauna (Čerňanský and Vasilyan 2024), the Walbeck amphibian and reptilian assemblage includes: 1) taxa known exclusively from the Palaeocene of Europe (e.g. *Wolterstorffiella*, *Venczelibatrachus, Camptognathosaurus*); 2) the first European appearances of Proteidae (*Geyeriella*), Salamandridae (*Koalliella*), Pelobatidae, and Lacertidae; and 3) two families, Palaeobatrachidae and Alytidae (*Venczelibatrachus*), with their roots in the Mesozoic (Fig. 11).

Further discoveries of new Palaeocene vertebrate sites will greatly contribute to the understanding of amphibian and also reptilian faunas from this epoch of the Cenozoic Era, as well as contribute to our understanding of the emergence, establishment, and palaeobiogeographic history of the present-day amphibian and reptilian clades on the Laurasian continents.

Supplementary Information The online version contains supplementary material available at https://doi.org/10.1007/s12549-025-00664-3.

Acknowledgements The authors would like to thank the guest editors of the special issue, Jim Gardner and Zoltán Szentesi, for the organisation of the issue and for their encouragement to contribute to the special issue. We thank Maximilian Albrecht and Roberto Rozzi (Natural Science Collections of the University of Halle-Saale) for their support in obtaining access to the material and Andrea Villa for critical discussion. We thank the handling guest editor Jim Gardner and the reviewers Annelise Folie, Zbyněk Roček, and Pavel Skutschas for thorough reviews and their valuable comments, improving the quality of the paper.

Funding The paper has been partially supported by the SNSF project nr. 200021_197323 (to DV). LM was funded by the Humboldt Foundation, through a Postodoctoral Fellowship.

Data availability The studied material is stored at the Institut für Geologische Wissenschaften und Geiseltalmuseum, Martin-Luther-Universität Halle-Wittenberg (MLU), Halle, Germany. All data generated or analysed during this study are included in this published article.

Declarations

Conflict of interest Authors declare no conflict of interest.

References

AmphibiaTree (2007). "*Rhyacotriton variegatus*" (On–line), Digital Morphology. Accessed April 16, 2025 at http://digimorph.org/specimens/Rhyacotriton_variegatus/whole/

Auffenberg, W. (1961). A new genus of fossil salamander from North America. *American Midland Naturalist, 66*(2), 456–465.

Augé, M. L., Duffaud, S., De Lapparent de Broin, F., Rage, J.-C., & Vasse, D. (1997). Les amphibiens et les reptiles de Prémontré (Cuisien, Bassin parisien): une herpétofaune de référence pour l'Eocène inférieur. *Géologie de la France, 1*, 23–33

Bailon, S. (1999). Différenciation ostéologique des Anoures (Amphibia, Anura) de France. *Fiches d'Ostéologie Animale pour l'Archéologie Série C: Varia, 1*, 3–41.

Bastir, M., Böhme, M., & Sanchiz, B. (2014). Middle Miocene remains of *Alytes* (Anura, Alytidae) as an example of the unrecognized value of fossil fragments for evolutionary morphology studies. *Journal of Vertebrate Paleontology, 34*(1), 69–79.

Batsch, A. J. G. K. (1788). *Versuch einer Anleitung, zur Kenntniß und Geschichte der Thiere und Mineralien, für akademische Vorlesungen entworfen, und mit den nöthigsten Abbildungen versehen, Erster Theil. Allgemeine Geschichte der Natur; besondre der Saügthiere, Vögel, Amphibien und Fische.* Jena: Akademische Buchhandlung.

Biton, R., Boistel, R., Rabinovich, R., Gafny, S., Brumfeld, V., & Bailon, S. (2016). Osteological observations on the alytid anura *Latonia nigriventer* with comments on functional morphology, biogeography, and evolutionary history. *Journal of Morphology, 277*(9), 1131–1145.

Blain, H. A., Canudo, J.-I., Cuenca-Bescós, G., & López-Martínez, N. (2010). Amphibians and squamate reptiles from the latest Maastrichtian (Upper Cretaceous) of Blasi 2 (Huesca, Spain). *Cretaceous Research, 31*(4), 433–446.

Blain, H. A., López-García, J. M., & Cuenca-Bescós, G. (2011). A very diverse amphibian and reptile assemblage from the late Middle Pleistocene of the Sierra de Atapuerca (Sima del Elefante, Burgos, Northwestern Spain). *Geobios*, *44*(2-3), 157–172.

Bonaparte, C. L. (1831). *Saggio di una distribuzione metodica degli animali vertebrati.* Rome: Antonio Bouzaler.

Bonaparte, C. L. (1850). *Conspectus systematum. Mastozoölogiae. Ornithologiae. Herpetologiae et Amphibiologiae. Ichthyologiae.* Rome: E. J. Brill, Lugduni Batavorum.

Buffetaut, E., Costa, G., Le Loeuff, J., Martin, M., Rage, J.-C-, Valentin, X., & Tong, H. (1996). An Early Campanian vertebrate fauna from the Villeveyrac Basin (Hérault, Southern France). *Neues Jahrbuch fur Geologie und Palaontologie Monatshefte, 1*, 1–16.

Čerňanský, A., & Vasilyan, D. (2024). Roots of the European Cenozoic ecosystems: lizards from the Palaeocene (~MP 5) of Walbeck in Germany. *Fossil Record, 27*(1), 159–186.

Cope, E. D. (1865). Sketch of the primary groups of Batrachia Salientia. *Natural History Review, 5,* 97–120.

De Bast, E., & Smith, T. (2016). The oldest Cenozoic mammal fauna of Europe: Implication of the Hainin reference fauna for mammalian evolution and dispersals during the Palaeocene. *Journal of Systematic Palaeontology, 15*(9), 741–785.

De Bast, E., Steurbaut, E., & Smith, T. (2013). New mammals from the marine Selandian of Maret, Belgium, and their implications for the age of the Palaeocene continental deposits of Walbeck. *Geologica Belgica, 16*(4), 236–244.

DeMar, D. G., Jr. (2013). A new fossil salamander (Caudata, Proteidae) from the Upper Cretaceous (Maastrichtian) Hell Creek Formation, Montana, U.S.A. *Journal of Vertebrate Paleontology, 33*(3), 588–598.

Denton, R. K., & O'Neill, R. C. (1998). *Parrisia neocesariensis*, a new batrachosauroidid salamander and other amphibians from the Campanian of eastern North America. *Journal of Vertebrate Paleontology, 18*(3), 484–494.

Edwards, J. L. (1976). Spinal nerves and their bearing on salamander phylogeny. *Journal of Morphology, 148*(3), 305–327.

Estes, R. (1976). Middle Palaeocene lower vertebrates from the Tongue River Formation, southeastern Montana. *Journal of Paleontology, 50*(3), 500–520.

Estes, R. (1981). Gymnophiona, Caudata. In P. Wellnhofer (Ed.), *Handbuch der Paläoherpetology – Encyclopedia of Paleoherpetology, Part 2* (pp. 1–115). Stuttgart, New York: Gustav Fischer.

Estes, R., & Sanchíz, B. (1982a). Early Cretaceous Lower Vertebrates from Galve (Teruel), Spain. *Journal of Vertebrate Paleontology, 2*(1), 21–39.

Estes, R., & Sanchíz, B. (1982b). New discoglossid and palaeobatrachid frogs from the Late Cretaceous of Wyoming and Montana, and a review of other frogs from the Lance and Hell Creek formations. *Journal of Vertebrate Paleontology, 2*(1), 9–20.

Estes, R., Hecht, M. K., & Hoffstetter, R. (1967). Palaeocene amphibians from Cernay, France. *American Museum Novitates, 2295*, 1–25.

Evans, S. E., & McGowan, G. J. (2002). Lissamphibian remains from the Purbeck Limestone Group, Southern England. *Special Papers in Palaeontology, 68*, 103–119.

Fischer, G. (1813). *Zoognosia. Tabulis Synopticis Illustrata, in Usum Prælectionum Academiæ Imperialis Medico—Chirurgicæ Mosquensis Edita, 3rd edn., vol 1.* Moscow: Typis Nicolai Sergeidis Vsevolozsky.

Fitzinger, L. (1843). *Systema Reptilium. Fasciculus Primus.* Wien: Braumüller et Seidel.

Gardner, J. D. (2003a). Revision of *Habrosaurus* Gilmore (Caudata; Sirenidae) and relationships among sirenid salamanders. *Palaeontology, 46(6)*, 1089–1122.

Gardner, J. D. (2003b) The fossil salamander *Proamphiuma cretacea* Estes (Caudata; Amphiumidae) and relationships within the Amphiumidae. *Journal of Vertebrate Paleontology, 23*(4), 769–782.

Gardner, J. D. (2008). New information on frogs (Lissamphibia: Anura) from the Lance Formation (Late Maastrichtian) and Bug Creek Anthills (Late Maastrichtian and Early Palaeocene), Hell Creek Formation, USA. In J. T. Sankey & S. Baszio (Eds.), *Vertebrate microfossil assemblages: their role in paleoecology and paleobiology* (pp. 219–249). Bloomington: Indiana University Press.

Gardner, J. D. (2012). Revision of *Piceoerpeton* Meszoely (Caudata: Scapherpetontidae) and description of a new species from the late Maastrichtian and ?early Palaeocene of western North America. *Bulletin de la Société Géologique de France, 183*(6), 611–620.

Gardner, J. D., & DeMar, D. G., Jr. (2013). Mesozoic and Palaeocene lissamphibian assemblages of North America: a comprehensive review. In J. D. Gardner & R. L. Nydam (Eds.), *Mesozoic and Cenozoic lissamphibian and squamate assemblages of Laurasia. Palaeobiodiversity and Palaeoenvironments, 93*(4), 459–515.

Gmelin, J. F. (1789). *Regnum animal. Caroli a Linne Systema Naturae per regna tri naturae, secundum classes, ordines, genera, species, cum characteribus, differentiis, synonymis, locis.* Leipzig: Beer.

Godinot, M., de Lapparent de Broin, F., Buffetaut, É., Rage, J.-C., & Russell, D. E. (1978). Dormaal: Une des plus anciennes faunes éocènes d´Europe. *Comptes Rendus hebdomadaires des Séances de l'Académie des Sciences, Série D: Sciences naturelles, 287*, 1273–1276

Goldfuss, G. A. (1820). *Handbuch der Zoologie, Bd. 2.* Nürnberg: J. L. Schrag.

Goloboff, P. A., Carpenter, J. M., Arias, J. S., & Esquivel, D. R. M. (2008). Weighting against homoplasy improves phylogenetic analysis of morphological data sets. *Cladistics*, *24*(5), 758–773.

Gómez, R. O., & Turazzini, G. F. (2015). An overview of the ilium of anurans (Lissamphibia, Salientia), with a critical appraisal of the terminology and primary homology of main ilial features. *Journal of Vertebrate Paleontology*, *36*(1), e1030023.

Gradstein, F. M., & Ogg, J. G. (2020). *Geologic time scale 2020*. Amsterdam: Elsevier.

Groessens-Van Dyck, M. C. (1981a). Etude des amphibiens du Montien continental de Hainin. *Bulletin de la Société belge de géologie, 90(2)*, 87–101.

Groessens-Van Dyck, M. C. (1981b). Note preliminaire sur les urodeles du gisement montien continental ed Hainin (Belgique). *Mémoires de l'Institut Géologique de l'Université de Louvain, 31*, 323–333.

Gubin, Y. M. (1991). Palaeocene salamanders from Southern Mongolia. *Paleontologicheskiy Zhurnal*, 1991, 96–106.

Haeckel, E. (1866). *Generelle Morphologie der Organismen.* Berlin: Georg Reimer.

Herre, W. (1939). Über die Urodelenreste von Walbeck. *Zeitschrift für Naturwissenschaften, 93(2),* 117–120.

Herre, W. (1950). Schwanzlurche aus dem Paleocän von Walbeck. *Zoologischer Anzeiger (Klatt-Festschrift)*, *145*, 286–301.

Herre, W. (1955). Die Fauna der miozänen Spaltenfüllung von Neudorf a.d. March (ČRS): Amphibia (Urodela). *Österreichische Akademie der Wissenschaften, Mathematisch-Naturwissenschaftliche Klasse Abteilung I, Sitzungsberichte, 164*, 783–803.

Ivanov, M. (2008). Early Miocene Amphibians (Caudata, Salientia) from the Mokrá-Western Quarry (Czech Republic) with comments on the evolution of Early Miocene amphibian assemblages in Central Europe. *Geobios, 41*(4), 465–492.

Jacisin, J. J., & Hopkins, S. S. (2018). A redescription and phylogenetic analysis based on new material of the fossil newts *Taricha oligocenica* Van Frank, 1955 and *Taricha lindoei* Naylor, 1979 (Amphibia, Salamandridae) from the Oligocene of Oregon. *Journal of Paleontology, 92*(4), 713–733.

Jetz, W., & Pyron, R. A. (2018). The interplay of past diversification and evolutionary isolation with present imperilment across the amphibian tree of life. *Nature Ecology & Evolution, 2*, 850–858.

Jia, J., Gao, K.-Q., Jiang, J.-P., Bever, G. S., Xiong, R., & Wei, G. (2021). Comparative osteology of the hynobiid complex *Liua—Protohynobius—Pseudohynobius* (Amphibia, Urodela): I. Cranial anatomy of *Pseudohynobius*. *Journal of Anatomy, 238*(2), 219–248.

Keeffe, R., & Blackburn, D. C. (2022). Diversity and function of the fused anuran radioulna. *Journal of Anatomy, 241*(4), 1026–1038.

Kuhn, O. (1940). Crocodilier und Squamatenreste aus dem oberen Paleocän von Walbeck. *Zentralblatt fuer Mineralogie, Geologie und Palaeontologie, Abteilung B, 1*, 21–25.

Linnaeus, C. (1758). *Systema naturae per regna tria naturae, secundum classes, ordines, genera, species, cum characteribus, differentiis, synonymis, locis.* Stockholm: L. Salvi.

Macaluso, L., Villa, A., Pitruzzella, G., Rook, L., Pogoda, P., Kupfer, A., & Delfino, M. (2020). Osteology of the Italian endemic spectacled salamanders, *Salamandrina* spp. (Amphibia, Urodela, Salamandridae): selected skeletal elements for palaeontological investigations. *Journal of Morphology*, *281*(11), 1391–1410.

Macaluso, L., Villa, A., & Mörs, T. (2022a). A new proteid salamander (Urodela, Proteidae) from the middle Miocene of Hambach (Germany) and implications for the evolution of the family. *Palaeontology*, *65*(1), e12585.

Macaluso, L., Mannion, P. D., Evans, S. E., Carnevale, G., Monti, S., Marchitelli, D., & Delfino, M. (2022b). Biogeographic history of Palearctic caudates revealed by a critical appraisal of their fossil record quality and spatio-temporal distribution. *Royal Society Open Science*, *9*(11), 220935.

Macaluso, L., Wencker, L. C., Castrovilli, M., Carnevale, G., & Delfino, M. (2023). A comparative atlas of selected skeletal elements of European urodeles (Amphibia: Urodela) for palae-ontological investigations. *Zoological Journal of the Linnean Society*, *197*(3), 569–619.

Maddison, W. P., & Maddison, D.R. (2023). Mesquite: a modular system for evolutionary analysis. Version 3.81 http://www.mesquiteproject.org

Mayr, G. (2002). An owl from the Palaeocene of Walbeck, Germany. *Fossil Record, 5*(11), 283–288.

Mayr, G. (2007). The birds from the Palaeocene fissure filling of Walbeck (Germany). *Journal of Vertebrate Paleontology, 27*(2), 394–408.

Naylor, B. G. (1978). The earliest known *Necturus* (Amphibia, Urodela), from the Palaeocene Ravenscrag Formation of Saskatchewan. *Journal of Herpetology, 12*(4), 565-569.

Naylor, B. G. (1979). The Cretaceous salamander *Prodesmodon* (Amphibia: Caudata). *Herpetologica, 35*(1), 11–20.

Noble, G. K. (1931). *The biology of the Amphibia*. New York: McGraw-Hill.

Přikryl, T., Aerts, P., Havelková, P., Herrel, A., & Roček, Z. (2009). Pelvic and thigh musculature in frogs (Anura) and origin of anuran jumping locomotion. *Journal of Anatomy, 214*(1), 100–139.

Pyron, R. A., & Wiens, J. J. (2011). A large-scale phylogeny of Amphibia including over 2800 species, and a revised classification of extant frogs, salamanders, and caecilians. *Molecular Phylogenetics and Evolution*, *61*(2), 543–583.

Rage, J. C. (2003). Oldest Bufonidae (Amphibia, Anura) from the Old World: a bufonid from the Palaeocene of France. *Journal of Vertebrate Paleontology*, *23*(2), 462–463.

Rage, J. C. (2012). Amphibians and squamates in the Eocene of Europe: what do they tell us? In T. Lehmann, & S. F. K. Schaal (Eds.), *Messel and the terrestrial Eocene - Proceedings of the 22nd Senckenberg Conference. Palaeobiodiversity and Palaeoenvironments*, *92*(4), 445–457.

Rage, J. C., & Augé, M. (2003). Amphibians and squamate reptiles from the lower Eocene of Silveirinha (Portugal). *Ciências da Terra (UNL)*, *15*, 103–116.

Rage, J. C., & Roček, Z. (2003). Evolution of anuran assemblages in the Tertiary and Quaternary of Europe, in the context of palaeoclimate and palaeogeography. *Amphibia Reptilia*, *24*(2), 133–168.

Ratnikov, V. Y., & Litvinchuk, S. N. (2007). Comparative morphology of trunk and sacral vertebrae of tailed amphibians of Russia and adjacent countries. *Russian Journal of Herpetology*, *14*(3), 177–190.

Ratnikov, V. Y., & Litvinchuk, S. N. (2009). Atlantal vertebrae of tailed amphibians of Russia and adjacent countries. *Russian Journal of Herpetology*, *16*(1), 57–68.

Roček, Z. (1981). Cranial anatomy of frogs of the family Pelobatidae Stannius, 1856, with outlines of their phylogeny and systematics. *Acta Universitatis Carolinae - Biologica, 1980*, 1–164.

Roček, Z. (1994). Taxonomy and distribution of Tertiary discoglossids (Anura) of the genus *Latonia* v. Meyer, 1843. *Geobios*, *27*(6), 717–751.

Roček, Z. (2013). Mesozoic and Tertiary Anura of Laurasia. . In J. D. Gardner & R. L. Nydam (Eds.), *Mesozoic and Cenozoic lissamphibian and squamate assemblages of Laurasia. Palaeobiodiversity and Palaeoenvironments*, *93*(4), 397–439.

Roček, Z., & Rage, J.-C. (2000). Tertiary Anura of Europe, Africa, Asia, North America, and Australia. In H. Heatwole & R. L. Carroll (Eds.), *Amphibian biology. Vol. 4. Palaeontology: the evolutionary history of amphibians* (pp. 1332–1387). Surrey Beatty & Sons: Chipping Norton.

Roček, Z., Wuttke, M., Gardner, J. D., & Singh Bhullar, B. A. (2014). The Euro-American genus *Eopelobates*, and a re-definition of the family Pelobatidae (Amphibia, Anura). *Palaeobiodiversity and Palaeoenvironments*, *94*(4), 529–567.

Roček, Z., Boistel, R., Lenoir, N., Mazurier, A., Pierce, S. E., Rage, J.-C., Smirnov, S. V., Schwermann, A. H., Valentin, X., Venczel, M., Wuttke, M., & Zikmund, T. (2015). Frontoparietal bone in extinct Palaeobatrachidae (Anura): its variation and taxonomic value. *The Anatomical Record*, *298*(11), 1848–1863.

Roček, Z., Rage, J. C., & Venczel, M. (2021). Fossil frogs of the genus *Palaeobatrachus* (Amphibia, Anura). *Abhandlungen der Senckenberg Gesellschaft für Naturforschung, 575*, 1–151.

Rose, C. S. (2003). The developmental morphology of salamander skulls. In H. Heatwole & D. Margaret (Eds.), *Amphibian biology. Vol. 5. Osteology* (pp. 1684–1781). Chipping Norton: Surrey Beatty & Sons.

Sanchiz, B. (1988). On the presence of zygosphene-zygantrum vertebral articulations in salamandrids. *Acta Zoologica Cracoviensia*, *31*(16), 493–504.

Sanchiz, B. (1998a). Salientia. In P. Wellnhofer (Ed.), *Handbuch der Paläoherpetologie–Encyclopedia of Paleoherpetology*, Part 4 (pp. 1–257). München: Verlag Dr. Friedrich Pfeil.

Sanchiz, B. (1998b). Vertebrates from the Early Miocene lignite deposits of the opencast mine Oberdorf (Western Styrian Basin, Austria). *Annalen des Naturhistorischen Museums in Wien*, *99*, 31–38.

Scopoli, G. A. (1777). *Introductio ad historiam naturalem, sistens genera lapidum, plantarum et animalium hactenus detecta, caracteribus essentialibus donata, in tribus divisa, subinde ad leges naturae.* Prague: Apud Wolfgangum Gerle.

Skutschas, P. P., & Gubin, Y. M. (2012). A new salamander from the late Palaeocene–early Eocene of Ukraine. *Acta Palaeontologica Polonica, 57*(1), 135–148.

Skutschas, P. P., Kolchanov, V. V., & Schwermann, A. H. (2020). First salamander from the Lower Cretaceous of Germany. *Cretaceous Research, 116*, 104606.

Skutschas, P. P., Malakhov, D. V., Parakhin, I. A., & Kolchanov, V. V. (2024). New data on the crown proteid *Bishara backa* from the Upper Cretaceous (Bostobe Formation) of Kazakhstan: implications for early evolution and palaeobiogeography of proteidae. *Historical Biology*, 1–9. https://doi.org/10.1080/08912963.2024.2384108

Smith, T., Quesnel, F., De Plöeg, G., De Franceschi, D., Metais, G., De Bast, E., Solé, F., Folie, A., Boura, A., Claude, J., Dupuis, C., Gagnaison, C., Iakovleva, A., Martin, J., Maubert, F., Prieur, J., Roche, E., Storme, J. Y., Thomas, R., Tong, H., Yans, J., & Buffetaut, E. (2014). First Clarkforkian equivalent land mammal age in the latest Palaeocene basal Sparnacian facies of Europe: fauna, flora, paleoenvironment and (bio) stratigraphy. *PLoS One*, *9(3)*, e86229.

Storch, G. (2008). Skeletal remains of a diminutive primate from the Palaeocene of Germany. *Naturwissenschaften, 95*(10), 927–930.

Szentesi, Z., & Venczel, M. (2012). A new discoglossid frog from the Upper Cretaceous (Santonian) of Hungary. *Cretaceous Research, 34*, 327–333.

Van Itterbeeck, J., Missiaen, P., Folie, A., Markevich, V. S., Van Damme, D., Dian-Yong, G., & Smith, T. (2007). Woodland in a fluvio-lacustrine environment on the dry Mongolian Plateau during the late Palaeocene: Evidence from the mammal bearing Subeng section (Inner Mongolia, PR China). *Palaeogeography, Palaeoclimatology, Palaeoecology*, *243*(1–2), 55–78.

Vasilyan, D. (2018). Eocene Western European endemic genus *Thaumastosaurus*: new insights into the question "Are the Ranidae known prior to the Oligocene?". *PeerJ*, *6*, e5511.

Vasilyan, D. (2020). Fish, amphibian and reptilian assemblage from the middle Miocene locality Gračanica—Bugojno palaeolake, Bosnia and Herzegovina. In U. B. Göhlich, & O. Mandic (Eds.), *The drowning swamp of Gračanica (Bosnia-Herzegovina) - a diversity hotspot from the middle Miocene in the Bugojno Basin. Palaeobiodiversity and Palaeoenvironments*, *100*(2), 437–455.

Vasilyan, D., & Yanenko, V. (2020). The last *Palaeoproteus* (Urodela: Batrachosauroididae) of Europe. *Scientific Reports, 10*, 2733.

Vasilyan, D., Zazhigin, V. S., & Böhme, M. (2017). Neogene amphibians and reptiles (Caudata, Anura, Gekkota, Lacertilia, and Testudines) from the south of western Siberia, Russia, and northeastern Kazakhstan. *PeerJ*, *5*, e3025.

Veith, M., Bogaerts, S., Pasmans, F., & Kieren, S. (2018). The changing views on the evolutionary relationships of extant Salamandridae (Amphibia: Urodela). *PLoS One*, *13(8)*, e0198237.

Venczel, M. (2000). Amphibians from the Lower Pleistocene Betfia 9 locality (Bihor county, Romania). *Satu Mare—Studii şi comunicări, seria stiintele naturale, 1*, 28–37

Venczel, M. (2004). Middle Miocene anurans from the Carpathian Basin. *Palaeontographica Abteilung A, 271(5–6)*, 151–174.

Venczel, M., & Codrea, V. A. (2018). A new proteid salamander from the early Oligocene of Romania with notes on the paleobiogeography of Eurasian proteids. *Journal of Vertebrate Paleontology*, *38(5)*, e1508027.

Venczel, M., & Hír, J. (2013). Amphibians and squamates from the Miocene of Felsőtárkány Basin, N-Hungary. *Palaeontographica Abteilung A*, *300*(1-6), 117–158.

Venczel, M., Gardner, J. D., Codrea, V. A., Csiki-Sava, Z., Vasile, Ş., & Solomon, A. A. (2016). New insights into Europe's most diverse Late Cretaceous anuran assemblage from the Maastrichtian of western Romania. In J. D. Gardner, & T. Přikryl (Eds.), *Contributions in honour of Zbyněk Roček. Palaeobiodiversity and Palaeoenvironments, 96*(1), 61–95.

Vergnaud-Grazzini, C., & Hoffstetter, R. (1972). Présence de Palaeobatrachidae (Anura) dans des gisements tertiaires Français. *Palaeovertebrata, 5*, 157–177.

Vergnaud-Grazzini, C., & Młynarski, M. (1969). Position systématic du genre *Pliobatrachus* Fejérváry 1917. *Comptes Rendus hebdomadaires des Séances de l'Académie des Sciences, Série D: Sciences naturelles, 268*, 2399–2402.

Villa, A., Roček, Z., Tschopp, E., Van Den Hoek Ostende, L. W., & Delfino, M. (2016). *Palaeobatrachus eurydices*, sp. nov. (Amphibia, Anura), the last western European palaeobatrachid. *Journal of Vertebrate Paleontology, 36*(6), e1211664.

Villa, A., Macaluso, L., & Mörs, T. (2024). Miocene and Pliocene amphibians from Hambach (Germany): New evidence for a late Neogene refuge in northwestern Europe. *Palaeontologia Electronica*, *27*(1), a3. https://doi.org/10.26879/1323

Wake, D. B. (1966). Comparative osteology and evolution of the lungless salamanders, family Plethodontidae. *Memoirs of the Southern Californian Academy of Sciences, 4*, 1–111.

Wake, D. B. (2001). "*Dicamptodon ensatus*" (On–line), Digital Morphology. Accessed April 16, 2025 at http://digimorph.org/specimens/Dicamptodon_ensatus/

Weigelt, J. (1939). Die Aufdeckung der bisher ältesten tertiären Säugetierfauna Deutschlands. *Nova Acta Leopoldina, Neue Folge, 4*, 515–528.

Weigelt, J. (1942). *Die alttertiären Säugetiere Mitteldeutschlands nach den Hallenser Grabungen im Geiseltal und bei Walbeck*. Berlin: De Gruyter.

Wilson, G. P., DeMar, D. G., & Carter, G. (2014). Extinction and survival of salamander and salamander-like amphibians across the Cretaceous-Palaeogene boundary in northeastern Montana, USA. In G. P. Wilson, W. A. Clemens, J. R. Horner & J. H. Hartman (Eds.), *Through the end of the Cretaceous in the type locality of the Hell Creek Formation in Montana and adjacent areas* (pp. 271–297). *Geological Society of America Special Paper, 503.*

Wuttke, M., Přikryl, T., Ratnikov, V. Y., Dvořák, Z., & Roček, Z. (2012). Generic diversity and distributional dynamics of the Palaeobatrachidae (Amphibia: Anura). *Palaeobiodiversity and Palaeoenvironments*, *92*(3), 367–395.